Defence Research and Development Canada
Recherche et développement pour la défense Canada

DRDC | RDDC
technologysciencetechnologie

Baseline predictions of BB2 submarine hydrodynamics for the NATO AVT-301 collaborative exercise

Mark C. Bettle
DRDC – Atlantic Research Centre

Defence Research and Development Canada
Scientific Report
DRDC-RDDC-2017-R200
March 2018

Canada

IMPORTANT INFORMATIVE STATEMENTS

This document was reviewed for Controlled Goods by DRDC using the Schedule to the *Defence Production Act*.

Disclaimer: Her Majesty the Queen in right of Canada, as represented by the Minister of National Defence ("Canada"), makes no representations or warranties, express or implied, of any kind whatsoever, and assumes no liability for the accuracy, reliability, completeness, currency or usefulness of any information, product, process or material included in this document. Nothing in this document should be interpreted as an endorsement for the specific use of any tool, technique or process examined in it. Any reliance on, or use of, any information, product, process or material included in this document is at the sole risk of the person so using it or relying on it. Canada does not assume any liability in respect of any damages or losses arising out of or in connection with the use of, or reliance on, any information, product, process or material included in this document.

Endorsement statement: This publication has been peer-reviewed and published by the Editorial Office of Defence Research and Development Canada, an agency of the Department of National Defence of Canada. Inquiries can be sent to: Publications.DRDC-RDDC@drdc-rddc.gc.ca.

© Her Majesty the Queen in Right of Canada, Department of National Defence, 2018

© Sa Majesté la Reine en droit du Canada, Ministère de la Défense nationale, 2018

Abstract

Initial predictions of the hydrodynamic loads and flow field for the generic BB2 submarine model were computed using the commercial viscous flow solver ANSYS CFX with the Baseline Reynolds stress turbulence model (BSL-RSM). A block structured mesh having 37×10^6 cells was created for this purpose. Calculations were performed at a Reynolds number of 9.57×10^6 for steady translation with zero flow incidence and at a drift angle of 10°. A strategy of alternating between large and small timesteps was found to be useful for converging the fluid equations for the wide range in time and length scales of vortices in the flow. The primary flow features around the BB2, such as junction vortices and appendage tip vortices, have been identified to guide future mesh improvements.

Significance for defence and security

Initial steps have been taken towards bench-marking and validating high fidelity tools for predicting submarine flow fields and manoeuvring forces. This is contributing to the assessment and improvement of our tools for understanding of submarine manoeuvring limitations in extreme conditions and for evaluating potential hydrodynamic performance improvements for submarines.

Résumé

Nous avons calculé les prévisions initiales des charges hydrodynamiques et du champ d'écoulement du modèle générique de sous-marin BB2 à l'aide du résolveur commercial d'écoulement visqueux ANSYS CFX et du modèle de référence de turbulence à contraintes de Reynolds (BSL-RSM). À cette fin, nous avons créé un maillage structuré multibloc de 37×10^6 cellules. Les calculs ont été effectués à un nombre de Reynolds de 9.57×10^6 selon une translation constante à débit nul et un angle de dérive de 10°. La stratégie qui consistait à alterner entre des intervalles de temps courts et longs s'est révélée utile à la convergence des équations des fluides dans une large gamme d'échelles de durées et de longueurs des tourbillons dans l'écoulement. Nous avons déterminé les principales caractéristiques de l'écoulement autour du BB2, telles que les tourbillons aux jonctions et à l'extrémité des appendices, ce qui orientera les améliorations à apporter au maillage à venir.

Importance pour la défense et la sécurité

Nous avons entrepris les premières étapes de l'établissement d'une référence et de la validation des outils à haute fidélité pour prévoir le champ d'écoulement de sous-marins et de leurs forces de manœuvre. Il s'agit d'une contribution à l'évaluation et à l'amélioration de nos outils servant à la compréhension des limites de manœuvre des sous-marins dans des conditions extrêmes, ainsi qu'à l'évaluation des améliorations possibles de la performance hydrodynamique des sous-marins.

Acknowledgements

The author would like to thank Serge Toxopeus, Maritime Research Institute Netherlands, for creating Figures 17 and 18 in this report.

Table of contents

Abstract i

Significance for defence and security i

Résumé ii

Importance pour la défense et la sécurité ii

Acknowledgements iii

Table of contents iv

List of figures vi

List of tables viii

1 Introduction 1

2 Geometry 1

3 Coordinate system 2

4 Flow conditions 3

5 Fluid domain and mesh 3

6 Viscous flow solver 9

7 Turbulence model 9

8 Boundary conditions 9

9 Discretization 10

10 Iterative convergence 10

11 Results and discussion 14

11.1 Flow Visualization 14

11.2 Zero Incidence flow field 15

11.3 Flow field for 10° drift case 20

11.4 Surface pressure and shear stress 22

11.5 Integrated Forces 25

12 Conclusions and future work 28

References 29

Annex A: ANSYS CFX solver settings for the 10 degrees drift angle case 31

Annex B: ANSYS CFX solver settings for the zero incidence case 42

List of figures

Figure 1: BB2 hull form (configuration 4) with coordinate system. 2

Figure 2: Block structure of DRDC's BB2 mesh (starboard half only). 5

Figure 3: Block edges on the symmetry plane. 5

Figure 4: Inflation layer blocks. 6

Figure 5: Grid on the BB2 surface and symmetry plane in the vicinity of the BB2. 7

Figure 6: Mesh cross section in the vicinity of the submarine at the aft end of the constant midbody section ($x/L_{pp} = -0.184$). 7

Figure 7: Maximum residuals for the continuity and momentum equations (top) and turbulence equations (bottom) during the zero incidence computation. . . 12

Figure 8: Maximum residuals for the continuity and momentum equations (top) and turbulence equations (bottom) during the $\beta = 10$ degrees computation. . 13

Figure 9: Percent difference between forces at iteration i and the forces at the end of the computation for the zero incidence computation. 14

Figure 10: Percent difference between forces at iteration i and the forces at the end of the computation for the $\beta = 10$ degrees computation. 15

Figure 11: Predicted vortex cores around the BB2 at zero incidence. 16

Figure 12: Centerplane ($y = 0$) cross section of the predicted sail-deck junction vortex for the zero incidence case. 18

Figure 13: Looking aft at vorticity contours on the $x = 0$ cross-sectional plane (located $0.060588L_{oa}$ aft of sail trailing edge) for the zero incidence case. 19

Figure 14: Predicted vortex cores around the BB2 at $\beta = 10°$. 21

Figure 15: Looking aft at vorticity contours on the $x = 0$ cross-sectional plane (located $0.060588L_{oa}$ aft of sail trailing edge) for the $\beta = 10°$ case. 23

Figure 16: Pressure through the primary sail tip vortex at midships ($x/L_{oa} = 0$) and the propeller plane ($x/L_{oa} = -0.481$), for the $\beta = 10°$ case. 24

Figure 17: Predicted pressure coefficient (top) and axial component of wall shear stress normalized by $0.5\rho U^2$ (bottom) along the BB2 for the zero incidence case. 26

Figure 18: Predicted pressure coefficient (top) and axial component of wall shear stress normalized by $0.5\rho U^2$ (bottom) along the BB2 for the $\beta = 10°$ case. 27

List of tables

Table 1: Main particulars of BB2 model (model scale 1:18.348). 2

Table 2: Flow conditions used for the simulations. 3

Table 3: Overall characteristics of the full mesh (after mirroring). 8

Table 4: Number of layers and cell spacing for the inflation layers shown in Figure 4. Layers start at the BB2 surface except OSo, which starts at the outer surface of OSi. 8

Table 5: Cell count and maximum spacing in various directions on the BB2 surface. 8

Table 6: Relaxation parameter settings. 11

Table 7: Location and magnitude of maximum vorticity in the core of the sail-deck junction vortices on the $y = 0$ plane upstream of the sail, shown in Figure 12. 17

Table 8: Location and magnitude of maximum x-component of vorticity in the core of the vortices on the $x = 0$ plane, shown in Figure 13 (starboard side only). 20

Table 9: Location and magnitude of maximum x-component of vorticity in the core of the vortices on the $x = 0$ plane, shown in Figure 15. 22

Table 10: Predicted BB2 hydrodynamic forces and moments for zero flow incidence, $Re_L = 9.57 \times 10^6$. 25

Table 11: Predicted BB2 hydrodynamic forces and moments for $\beta = 10°$, $Re_L = 9.57 \times 10^6$. 25

1 Introduction

The NATO AVT-301 working group, "Flow field prediction for manoeuvring underwater vehicles", is using the generic BB2 submarine geometry [1] for a benchmark study assessing the ability of viscous flow solvers to predict the hydrodynamic performance of a manoeuvring submarine. The objective is to improve awareness of modelling requirements and/or shortfalls by comparing CFD codes and methods, and by validating predictions against experimental data. An equally important objective is to gain a deeper understanding of the fluid dynamics of a manoeuvring submarine through this process. Three submarine motions are planned for this benchmarking activity: straight flight (zero flow incidence), steady drift, and constant turning rate manoeuvres. Wind tunnel data will be provided by Defence Science and Technology Group (DSTG) in Australia and rotating arm data will be provided by QinetiQ in the UK for comparison.

For phase 0 of this collaborative exercise, participants performed initial flow field computations of the BB2 at straight flight and at a steady drift angle of 10 degrees using their own methods and best practices. The purpose of this phase is to get an initial indication of the variation in predicted quantities due to the use of different codes, meshes, turbulence models, etc. This comparison will provide direction for the aspects that should be studied in further detail. The instructions and additional details for this test case were given by Toxopeus and Kerkvliet [2]. The following output quantities are being compared: hydrodynamic forces and moments, shear stress and pressure distributions on the BB2 surface, and flow field quantities at different cross-sections, including: velocity, vorticity, pressure, and turbulent kinetic energy.

Defence Research and Development Canada (DRDC) performed Reynolds-Averaged Navier-Stokes (RANS) computations with the commercial code ANSYS CFX for phase 0 of this collaborative exercise. The purpose of this document is to describe the details of the mesh, boundary conditions, solver settings, turbulence model, and convergence for these computations. Some of the key results are also presented, but a more detailed analysis including a comparison with submissions from other participants will be documented in a separate report.

2 Geometry

The generic BB2 hull form is shown in Figure 1 and the main particulars are given in Table 1. This geometry was designed by the Maritime Research Institute Netherlands (MARIN) [1] by modifying the BB1 submarine geometry, which in turn was devised based on a concept design by Joubert [3]. MARIN conducted free running model tests with the BB2 hullform, as described by Overpelt et. al [1]. The BB2 geometry is available on the MARIN website at `http://www.marin.nl/web/Ships-Structures/Navy/Submarines.htm`. Four configurations of the BB2 have been defined: hull with deck (configuration 1); hull with deck and sail (configuration 2); hull with deck, sail, and tail planes (configuration 3);

and hull with deck, sail, tail planes, and sailplanes (configuration 4). The letter "P" is appended to the configuration number if the propeller is included. The fully appended hull without propeller (configuration 4) was used for this work. Note that the geometry is given in full-scale dimensions but it was scaled to the model scale length for the present study.

Table 1: *Main particulars of BB2 model (model scale 1:18.348).*

Quantity	Symbol	Value		Unit
		Full	Model	
Length overall	L_{oa}	70.2	3.8260	m
Beam	B	9.6	0.5232	m
Depth (to deck)	D	10.6	0.5777	m
Depth (to top of sail)	D_{sail}	16.2	0.8829	m

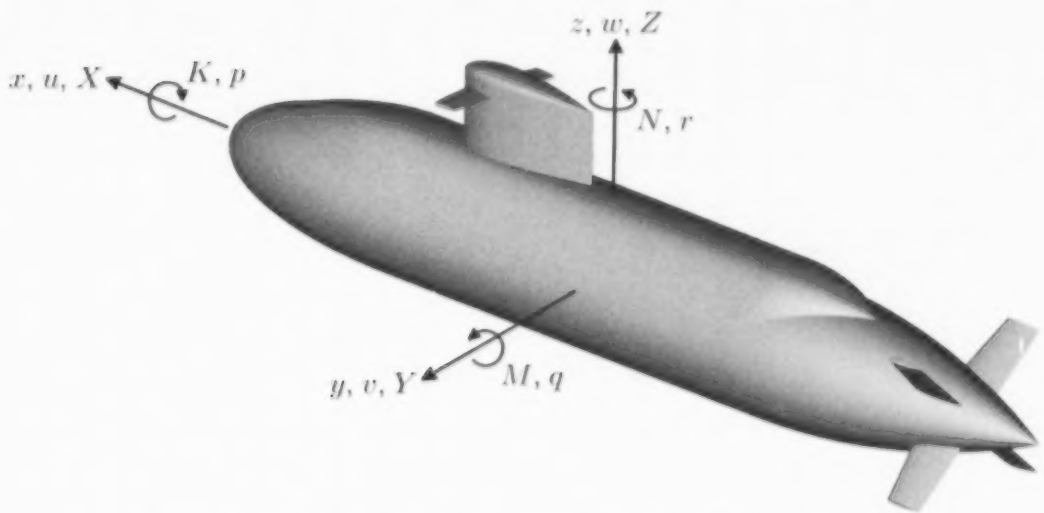

Figure 1: *BB2 hull form (configuration 4) with coordinate system.*

3 Coordinate system

The primary coordinate system was set to have the origin located on the hull axis at midships (located 1.913 m aft of the nose of the submarine at model scale). As shown in Figure 1, the positive x axis is directed forward through the nose, the y axis to port, and z axis vertically upward. The submarine velocity components in the x, y, and z directions are denoted as u, v, and w, and the submarine rotational velocities about these axes are given by p, q, and r. The present study only considers pure translation in the xy plane, such that $w = p = q = r = 0$. The drift angle is defined by $\beta = \arctan(v/u)$, which means β is positive for flow coming from port side.

All forces X,Y,Z and moments K,M,N were directed as shown in Figure 1 and made non-dimensional as follows:

$$X',Y',Z' = \frac{X,Y,Z}{\frac{1}{2}\rho U^2 L_{oa}^2} \qquad K',M',N' = \frac{K,M,N}{\frac{1}{2}\rho U^2 L_{oa}^3} \tag{1}$$

where ρ is fluid density, $U = \sqrt{(u^2+v^2+w^2)}$ is the submarine speed, and L_{oa} is the overall length of the submarine (see Table 1).

A second coordinate system, $\tilde{x},y,z$, is used for the flow field data. It is the same as the primary coordinate system for hydrodynamic loads except the origin is shifted to the aft perpendicular, such that $\tilde{x} = x + L_{oa}/2$.

4 Flow conditions

The flow properties used for the computations are given in Table 2. Computations were performed for drift angles of $\beta = 0$ and $\beta = 10°$ (flow from port side). The Reynolds number based on submarine length, Re_L, was set to 9.57×10^6 by using the model scale submarine length (3.826 m), a free stream speed of 3 m/s, a water density of 1000 kg/m^3, and kinematic viscosity of 1.2×10^{-6} m^2/s.

Table 2: *Flow conditions used for the simulations.*

Quantity	Symbol	Value(s)
Inflow speed	$V_\infty = U$	3 m/s
Drift angles	β	0°, 10°
Inflow velocity in x-dir	V_x	$-V_\infty \cos(\beta)$
Inflow velocity in y-dir	V_y	$-V_\infty \sin(\beta)$
Inflow velocity in z-dir	V_z	0
Density	ρ	1000 kg/m^3
Viscosity	ν	1.2×10^{-6} m^2/s
Reynolds Number	Re_L	9.57×10^6

5 Fluid domain and mesh

A rectangular box was used for the fluid domain around the BB2 model, with upstream face at $x = 2.5L_{oa}$, downstream face at $x = -3.5L_{oa}$, and sides and top at $y,z = \pm 2L_{oa}$. These distances were selected based on a RANS verification and validation study of asymmetric hulls by Baker [4], which showed that a nominal distance of $2L_{oa}$ between the hull and far field boundaries was adequate.

A block structured mesh was created with the commercial software Pointwise v18.0R2 for

the starboard half of the fluid domain using full scale dimensions in millimetres. This half mesh was then mirrored about $y = 0$ and scaled to model scale dimensions ($L_{pp} = 3.826$ m) using the pre-processing tool ANSYS CFD Pre v17.1. This process ensured that the full mesh was symmetric about the BB2 centre plane.

Figures 2, 3 and 4 show, respectively, the block structure for the overall mesh, the edges of the blocks on the symmetry plane, and the inflation layer O-grids surrounding the BB2. In the full mesh (after mirroring) there are 476 blocks and 36,952,960 hexahedral cells. Figure 5 shows the mesh on the submarine surface and plane of symmetry in the vicinity of the submarine and Figure 6 shows a cross-section of the near-body portion of the mesh at the longitudinal position where the hull begins to taper ($x/L_{pp} = -0.184$). An inflation layer having a thickness of approximately 2 meters full scale (0.11 m at model scale) surrounds the BB2 hull. The height of the first cell off the BB2 surface was set to 8.5×10^{-6} meters full scale (4.63×10^{-7} meters model scale), which yields a low average y^+ value of less than 0.05 for these calculations. The wall-normal mesh expansion rate at the BB2 surface was 1.12. Table 3 gives a summary of mesh parameters and metrics, Table 4 give the number of layers and cell spacing for the inflation layer blocks around the BB2, and Table 5 gives the number of cells and maximum spacing in various directions along the BB2 hull and appendages.

It required considerable effort—on the order of two to three months—to create and adjust the block structured mesh around the appended submarine model. An unstructured mesh with tetrahedral cells could have been generated in much less time. However, a study by Hally [5] showed that tetrahedral cells cause excessive diffusion in propagating vortices even when using as many as 22 cells across the vortex core. In contrast, hexahedral cells were found to resolve the vortex core pressure and circumferential velocity distribution using on the order of 10 cells across the core, when the cells are aligned with the axis of the vortex. Achieving the same accuracy with tetrahedral cells would require a very large number of cells and likely more computational resources than are currently available at DRDC. Additional meshing approaches should be explored in follow-on studies, such as the use of a hybrid mesh where hexahedral cells are used in the boundary layer and where there are vortices but unstructured cells are used elsewhere to reduce the effort of mesh generation.

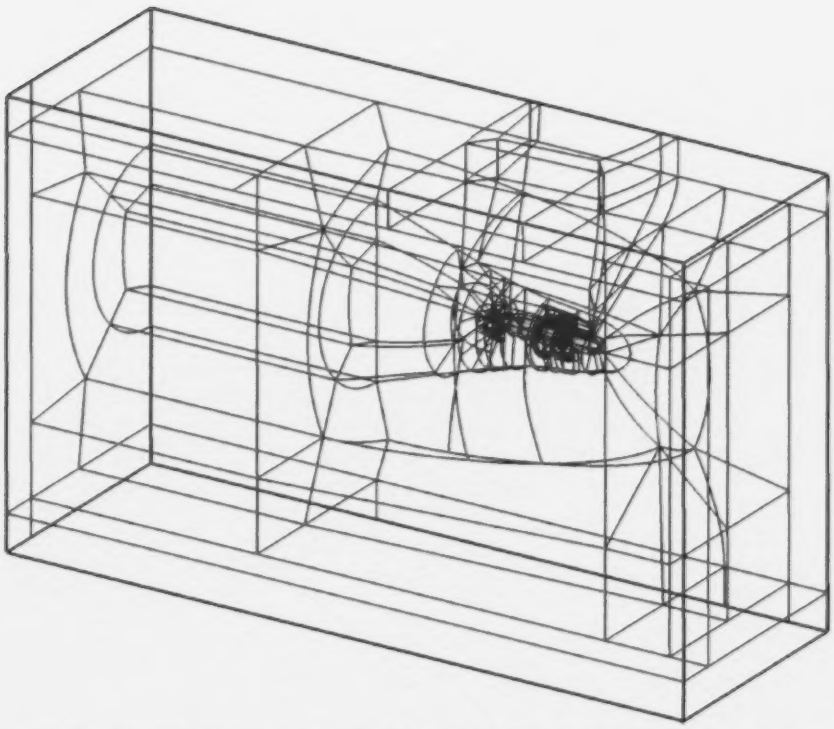

Figure 2: *Block structure of DRDC's BB2 mesh (starboard half only).*

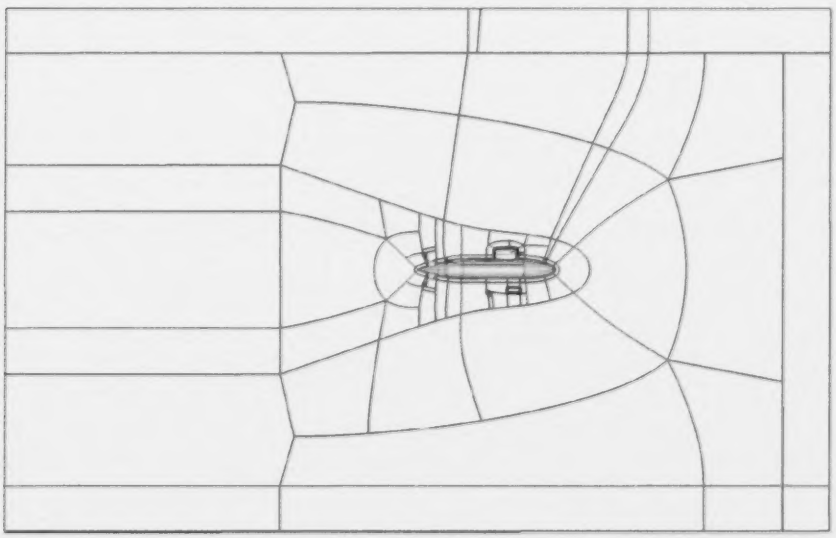

Figure 3: *Block edges on the symmetry plane.*

Figure 4: *Inflation layer blocks.*

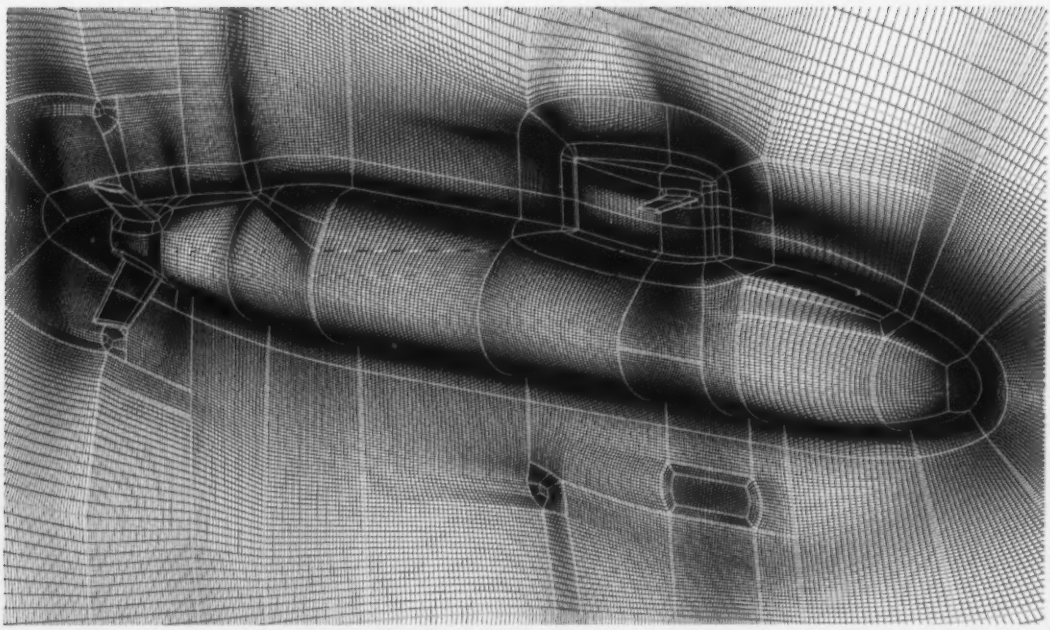

Figure 5: *Grid on the BB2 surface and symmetry plane in the vicinity of the BB2.*

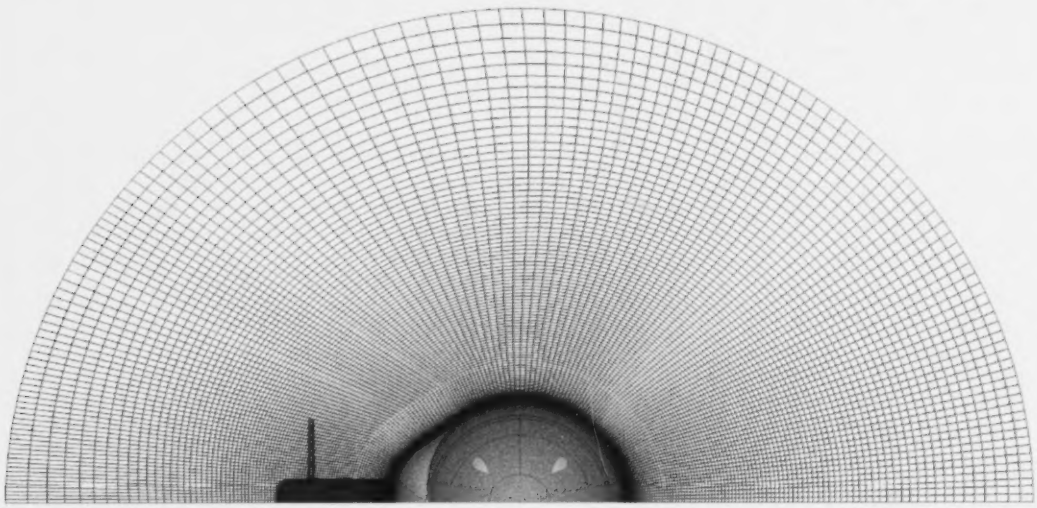

Figure 6: *Mesh cross section in the vicinity of the submarine at the aft end of the constant midbody section* ($x/L_{pp} = -0.184$).

Table 3: *Overall characteristics of the full mesh (after mirroring).*

Total mesh cells (hexahedral)	36,952,960
Submarine surface faces (quadrilateral)	371,616
Height of first cell at BB2 surface	$1.21 \times 10^{-7}\, L_{oa}$
Wall-normal expansion rate at BB2 surface	1.12
Minimum internal cell angle	39.2 deg
Maximum aspect ratio	75,181
Maximum volume ratio between adjacent cells	3.24

Table 4: *Number of layers and cell spacing for the inflation layers shown in Figure 4. Layers start at the BB2 surface except OSo, which starts at the outer surface of OSi.*

Inflation Layer	Thickness full scale (m)	# of layers (cells)	Start Spacing full scale (mm)	End Spacing full scale (mm)	Expansion Rate (start)
Hull (OH)	2.0	96	0.0085	125	1.12
Sail Inner (OSi)	1.0	160	0.0085	37.5	1.07
Sail Outer (OSo)	3.2	36	37.5	88 - 250	1.05
Sail plane (OSP)	0.45	72	0.0085	80	1.13
Tail planes (OT*)	0.9 - 2.7	72	0.0085	90 - 375	1.11 - 1.13

Table 5: *Cell count and maximum spacing in various directions on the BB2 surface.*

Direction	# of cells	Max. spacing
Longitudinal, nose to tail	416	0.0085 L_{oa}
Circumferential (360°): midbody	264	0.0078 πB
Circumferential (360°): nose, tail	240	0.013 πD_{local}
Sail, chordwise (one side)	168	0.037 C_{sail}
Sail, spanwise (one side)	144	0.035 S_{sail}
Sail plane, chordwise (one side)	56	0.054 C_{sp}
Sail plane, spanwise (one side)	188	0.045 S_{sp}
Tail plane, chordwise (one side)	56	0.058 C_{tp}
Tail plane, spanwise (one side)	128	0.026 S_{tp}

6 Viscous flow solver

The commercial viscous flow solver ANSYS CFX v17.1 was used for these calculations. ANSYS CFX solves the Navier-Stokes equations using a strong conservation formulation. It has several models for turbulence, including Reynolds-Averaged Navier-Stokes (RANS) based models as well as Large Eddy Simulation (LES) and Detached Eddy Simulation (DES) models. The incompressible steady RANS equations with a Reynolds stress model (described below) were used for the present simulations.

ANSYS CFX uses an element-based finite-volume method to solve the discretized continuity and momentum equations. All fluid solution variables are stored at the mesh vertices (nodes). Reference [6] describes how control volumes are constructed around the nodes and where integration points are located for evaluating control volume surface fluxes. Tri-linear finite element shape functions are used to interpolate quantities at the integration points.

ANSYS CFX uses a coupled solver [7, 8] to solve the hydrodynamic equations (for u, v, w, p) as a single system and the Additive Correction [9] Algebraic Multi-grid [10] procedure is used to accelerate the solution.

7 Turbulence model

The Baseline Reynolds stress model (BSL-RSM) implemented in ANSYS CFX v17.1 [6] was used for these calculations. This model solves six transport equations for the Reynolds stresses and one equation for the turbulent eddy frequency ω. The mathematical formulation for the BSL-RSM is given in Reference [6].

The Reynolds stress model inherently models anisotropies in the Reynolds stresses, unlike two equation turbulence models based on a Boussinesq relationship which assumes isotropic turbulence. A study by Jeans et al. [11] showed that the BSL-RSM better predicted the normal force on the DRDC-STR and Series 58 submarine hullforms at incidence compared to the two equation $k-\omega$ SST turbulence model. The SST normal force predictions under-predicted the BSL-RSM and experimental results due to delayed separation and a less concentrated leeside vortex, resulting in less energy loss.

The disadvantage of using the BSL-RSM model over the SST and other two equation models is increased computational requirements and (generally) less robustness.

8 Boundary conditions

The location of the far field boundaries is given in Section 5. The following boundary conditions were applied for the calculations:

- The BB2 submarine surface was given a smooth, no-slip wall boundary condition.

- The far-field boundaries that are nominally tangent to the free stream flow (top, bottom, and sides at zero incidence; top and bottom at $\beta = 10°$) were given the "Opening for Entrainment" boundary condition. For this condition, the pressure is set to zero, and the gradients of velocity and turbulent quantities perpendicular to the boundary were set to zero. Flow can either enter or leave these boundaries as determined implicitly from the solution.
- On boundaries where the free stream flow is known to only enter the domain (forward boundary at zero incidence; forward and port-side boundaries at $\beta = 10°$), the inflow velocity components are specified, the turbulent intensity is set to 1% and the ratio of turbulent viscosity (μ_t) to dynamic viscosity (μ) is set to 1.
- On the boundaries where the flow is only leaving the domain (aft boundary at zero incidence; aft and starboard side boundaries at $\beta = 10°$) the average pressure over the whole boundary was constrained to zero. The pressure varies spatially over the boundary, as determined implicitly by the solution, but the average pressure is zero on each outlet face.

9 Discretization

The discretized momentum and continuity equations were solved using a method that is formally second order accurate in space. The following second-order upwind scheme was used for the advection term:

$$\phi_{ip} = \phi_{up} + \beta \nabla \phi \cdot \Delta r \tag{2}$$

where ϕ_{ip} is the quantity evaluated at the integration point (for computing the surface integral), ϕ_{up} is the quantity at the upwind node, r is the vector from the upwind node to the integration point, and β is a blend factor. The gradient $\nabla\phi$ was set equal to the average of the adjacent nodal gradients and the blend factor β was set to 1 to achieve second order accuracy.

The first order upwind scheme was used for the advection terms in the turbulence equations.

10 Iterative convergence

A pseudo time step was used in ANSYS CFX to converge the RANS equations to a steady solution. It was found that the most efficient method for converging to a steady solution was to alternate between a larger time step and a small time step. The large time step was required to quickly achieve a global solution for the large length scales, but it does not provide enough stability to converge regions of small scale eddies / high vorticity, such as at the horseshoe vortex around the sail-deck junction described in Section 11.2. The small time step provides a stable solution, but the convergence is very slow globally. The following procedure was found to provide a reasonably efficient solution:

1. Run N time steps (iterations) with the large time step ($\Delta t_{lg} = \frac{1}{50} L_{oa}/U$), where N was set to 200 for the zero incidence case and 500 for the $\beta = 10$ degrees case;

2. Alternate between 300 iterations with the small time step ($\Delta t_{sm} = \frac{1}{5000} L_{oa}/U$) and 15 iterations with Δt_{lg} until the L_∞ norm (maximum) residuals drop to the specified convergence criteria.

In addition to varying the pseudo time step size, the relaxation parameters in Table 6 were set to help achieve stable iterative convergence. All ANSYS CFX solver settings and boundary conditions used for the 10 degrees drift and zero incidence cases are shown in Annex A and Annex B, respectively.

Table 6: *Relaxation parameter settings.*

Parameter	Setting for case $\beta = 0°$	Setting for case $\beta = 10°$
`Gradient Relaxation`	`0.01`	`0.1`
`relax mass`	`0.4`	`0.4`

Figures 7 and 8 show the normalized maximum (L_∞) residuals for the zero incidence and 10 degree drift cases, respectively. The sudden periodic changes in residuals are a result of the changes in timestep size. In both cases, the maximum residuals in the entire fluid domain for all equations were reduced to 3×10^{-5} by the end of the simulations. The zero incidence case required 3,630 iterations whereas the $\beta = 10°$ case required 2,000 iterations. Note that the faster convergence for the steady drift case was probably achieved because more large time steps are used initially (before alternating between small and large time steps) and a larger value was used for `Gradient Relaxation` (meaning less under-relaxation was applied).

The convergence of hydrodynamic forces for the zero incidence and 10 degree drift cases are shown in Figure 9 and Figure 10, respectively. All forces vary by less than 0.1% during the last 900 iterations of the zero incidence case and by less than 0.03% during the final 900 iterations in the $\beta = 10$ degrees case.

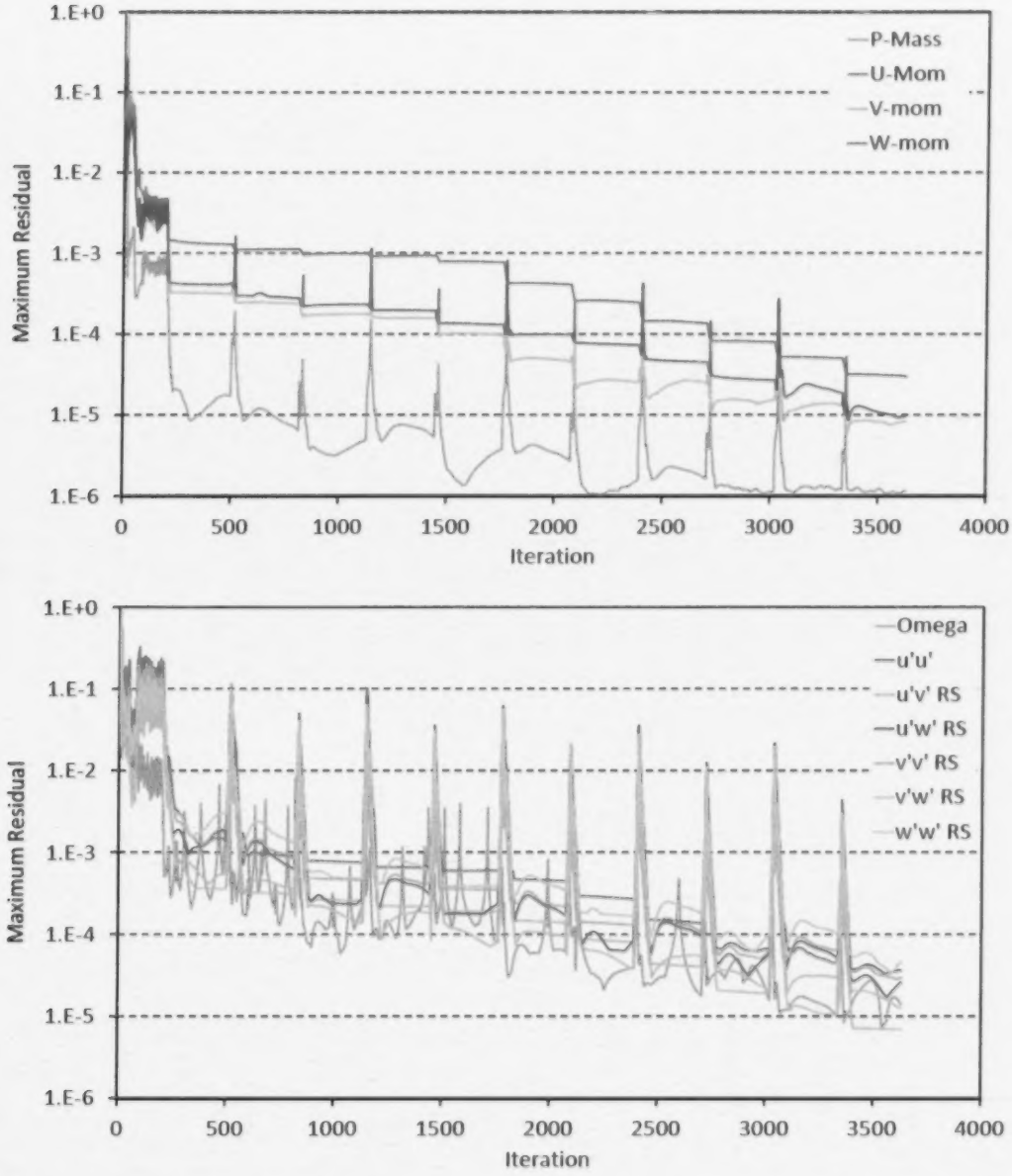

Figure 7: *Maximum residuals for the continuity and momentum equations (top) and turbulence equations (bottom) during the zero incidence computation.*

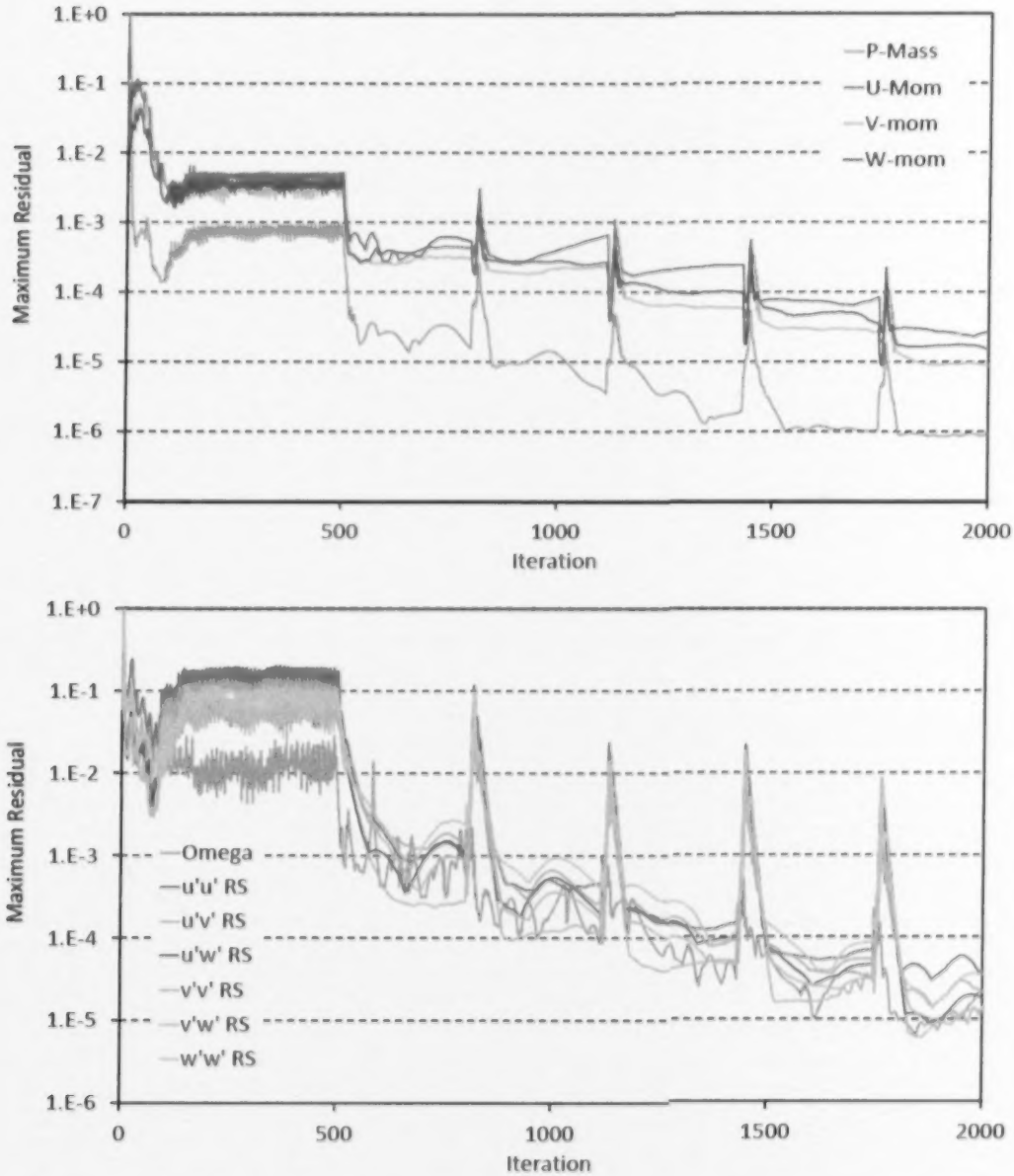

Figure 8: *Maximum residuals for the continuity and momentum equations (top) and turbulence equations (bottom) during the* $\beta = 10$ *degrees computation.*

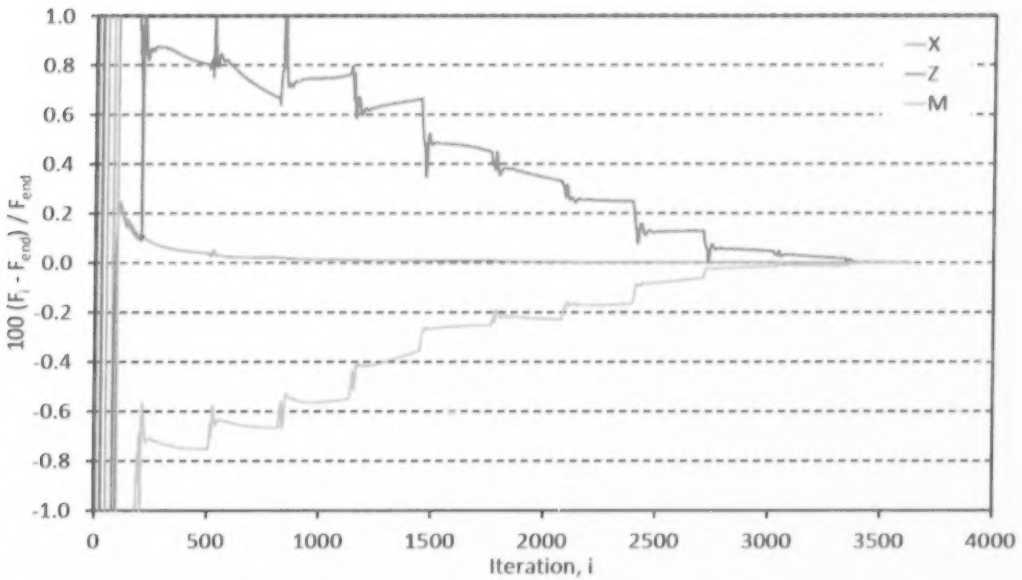

Figure 9: *Percent difference between forces at iteration i and the forces at the end of the computation for the zero incidence computation.*

11 Results and discussion

11.1 Flow Visualization

Following Toxopeus et al. [12], the vortices in the flow around the BB2 are visualized using iso-surfaces of constant Q-values, defined as follows:

$$Q = \frac{1}{2}\left(|\Omega|^2 - |S|^2\right) \tag{3}$$

where $\Omega = \left(\nabla\mathbf{u} - \nabla\mathbf{u}^T\right)/2$ is the vorticity tensor and $S = \left(\nabla\mathbf{u} + \nabla\mathbf{u}^T\right)/2$ is the strain tensor. In this work, Q is made non-dimensional as follows:

$$Q' = Q\left(\frac{L_{oa}}{V_\infty}\right)^2 \tag{4}$$

The Q iso-surfaces are colored by non-dimensional helicity, H', in order to indicate the direction or rotation:

$$H' = \frac{\omega \cdot \mathbf{u}}{|\omega||\mathbf{u}|} \tag{5}$$

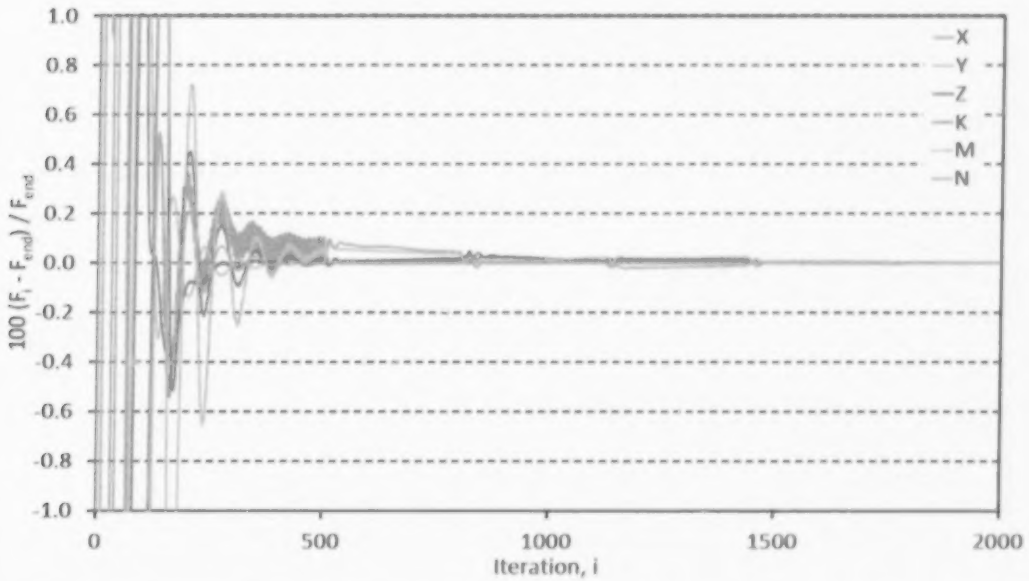

Figure 10: *Percent difference between forces at iteration i and the forces at the end of the computation for the $\beta = 10$ degrees computation.*

where ω is the local vorticity vector and $\mathbf{u}$ is the local velocity vector. Normalized helicity indicates the angle between the velocity vector and the vorticity vector; $H' = 1$ when velocity and vorticity vectors are pointing in the same direction and $H' = -1$ when they are pointing in opposite directions. Thus as the vortices tend to align with the flow after they leave the body, H' tends towards ± 1, with positive values indicating a clockwise rotation and negative values indicating counter-clockwise rotation when looking in the direction of the flow.

11.2 Zero Incidence flow field

Figure 11 shows the predicted primary vortices around the BB2 for the zero incidence. There are pairs of counter-rotating vortices shed from the tips of the sail, sailplanes, and tail planes. There are also horseshoe vortex systems generated upstream of each appendage-hull junction and the sailplane-sail junction. These vortices wrap around each appendage and propagate towards the aft end of the submarine. The legs of the sailplane horseshoe vortices propagate to the trailing edge of the sail, where they then leave the sail and propagate aftwards, just below the primary sail tip vortices. In a similar manner, the legs of the tail plane junction vortices propagate to the end of the submarine and separate off the hull near the after perpendicular.

Figure 11: *Predicted vortex cores around the BB2 at zero incidence.*

The sail-deck junction vortex system is the largest and it is predicted to remain coherent until near the end of the deck casing. Details of the predicted sail junction vortex system are shown on the submarine plane of symmetry, just upstream of the sail in Figure 12. The flow separates from the deck as it approaches the 90° corner between the deck and the leading edge of the sail. There is a strong reversed flow region in front of the leading edge of the sail, which rolls up into the primary vortex at around $\tilde{x}/L_{oa} = 0.721$. There are additional weaker secondary vortices predicted forward of this primary vortex. The location and magnitude of peak vorticity in the y direction, ω_y, at each of these three vortex cores is tabulated in Table 7. The dimensions of this vortex system are small relative to the overall submarine, with the diameter of the primary core predicted to be approximately 0.1% of the submarine length. It required a few iterations in the meshing process to place enough mesh cells to resolve the features shown in Figure 12 (note that there is a mesh node at the tail of each velocity vector in this figure). Even further refinement may be needed to converge the magnitude of vorticity at the core.

Table 7: *Location and magnitude of maximum vorticity in the core of the sail-deck junction vortices on the $y = 0$ plane upstream of the sail, shown in Figure 12.*

Vortex #	$\tilde{x}/L_{oa}$	z/L_{oa}	$\omega_y\ L_{oa}/V_\infty$ Max/Min
1	0.72082	0.08359	-3594
2 [a]	0.72193	0.083049	1186
3	0.72356	0.08306	-711.0

[a] No local max for ω_y in vortex 2 due to boundary layer interaction; values are for the zero velocity point at the core.

Figure 13 shows a lateral cross section of vortices at $x = 0$ ($0.060588 L_{oa}$ aft of sail trailing edge) for the zero incidence case. The numbering of vortices is consistent with Figure 12; vortex 1 is the primary sail-deck junction vortex and vortices 2 and 3 are the secondary sail-deck junction vortices. Note that due to symmetry, there are vortices of equal strength but opposite rotation on each side of the $y = 0$ centre plane. Directly behind the sail, there are an additional 9 predicted vortices on each side of the centre plane (labelled 4-12). The top vortices — the strongest of the group — were generated at the sail tip. Below that, there are 4 sets of vortices on each side of the centre plane which originate from the junction between the sailplane and the sail. Further down, behind the root of the sail, there are an additional 4 pairs of vortices, with the bottom pair being the strongest. Finally, the vortex labelled 13 in Figure 13 is the tip vortex from the sailplanes. The cores of each of these vortices at $x = 0$ are identified by the local peak in the axial component of vorticity, ω_x, as tabulated in Table 8.

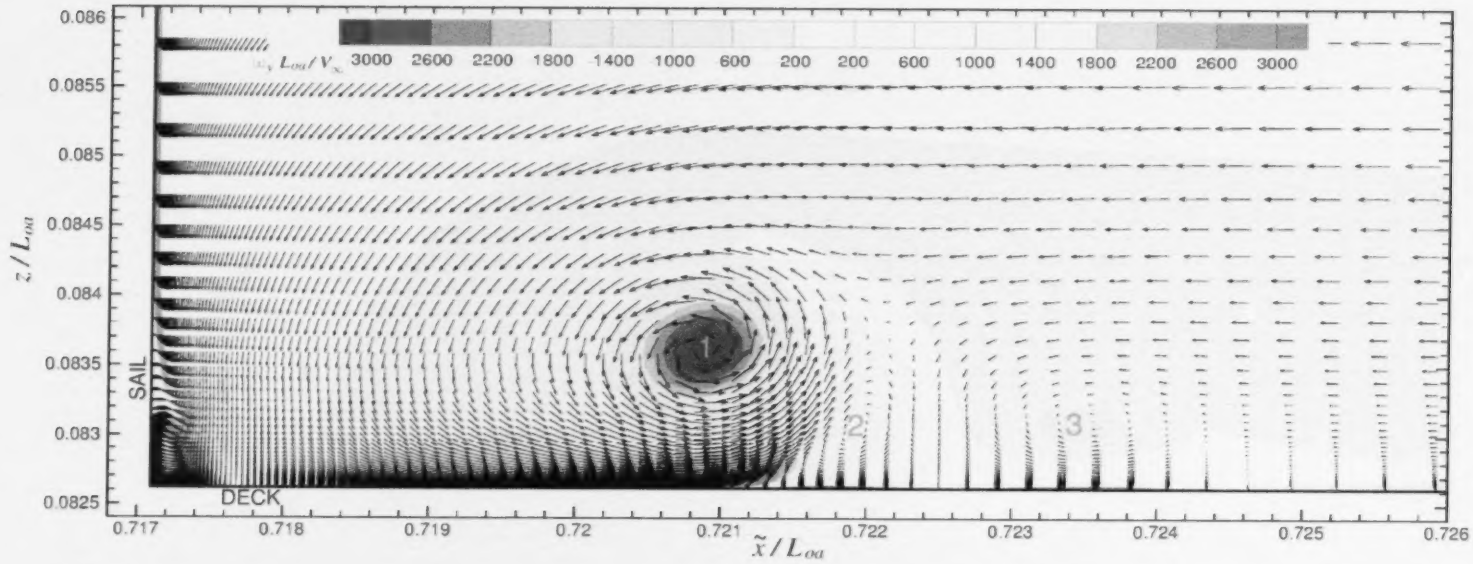

Figure 12: *Centerplane ($y = 0$) cross section of the predicted sail-deck junction vortex for the zero incidence case.*

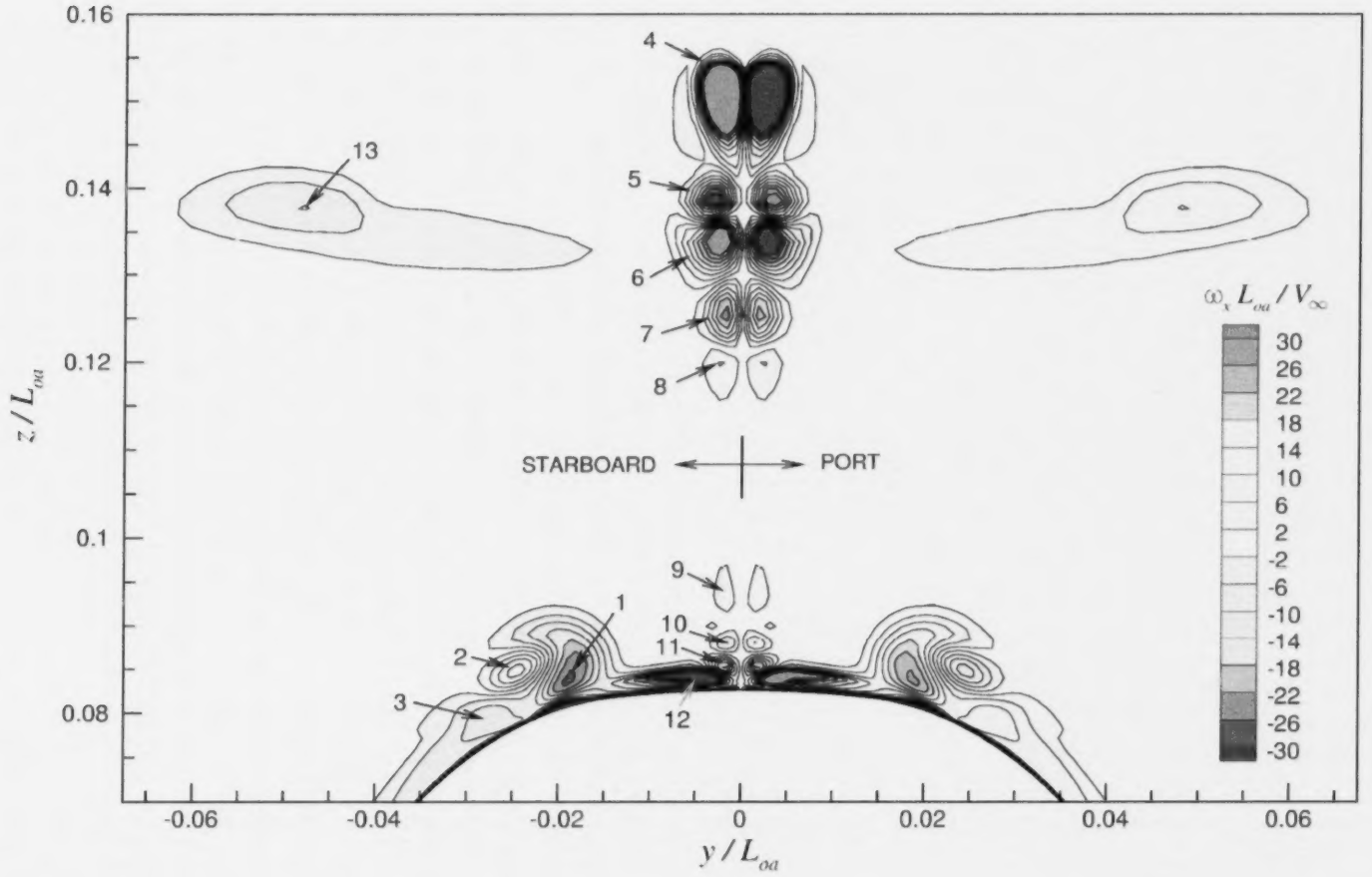

Figure 13: *Looking aft at vorticity contours on the $x = 0$ cross-sectional plane (located $0.060588 L_{oa}$ aft of sail trailing edge) for the zero incidence case.*

Table 8: *Location and magnitude of maximum x-component of vorticity in the core of the vortices on the $x = 0$ plane, shown in Figure 13 (starboard side only).*

Vortex #	y/L_{oa}	z/L_{oa}	$\omega_x\ L_{oa}/V_\infty$ Max/Min
1	-0.01853	0.08433	-26.69
2	-0.02431	0.08495	15.88
3	-0.02777	0.07964	-12.81
4	-0.00267	0.15166	95.29
5	-0.00350	0.13847	-36.51
6	-0.00259	0.13370	43.55
7	-0.00168	0.12522	-24.45
8	-0.00252	0.11991	6.25
9	-0.00156	0.09352	-3.31
10	-0.00151	0.08807	-10.18
11	-0.00148	0.08521	22.72
12	-0.00378	0.08389	-56.96
13	-0.04794	0.13771	-10.19

11.3 Flow field for 10° drift case

Figure 14 shows the predicted primary vortices for the $\beta = 10°$ case. In this case, there is a strong sail tip vortex that rotates counter-clockwise when looking in the direction of the flow. This is expected from theory as the sail acts as a wing in cross flow. There is also a strong vortex (H1 in Figure 14) separating from the lee side (in this case the starboard side) of the hull and propagating downstream between the rudders on the starboard side of the BB2. This primary hull vortex rotates in the opposite direction of the sail tip vortex. A second, weaker hull vortex, H2, rotates in the opposite sense as H1. vortices H1 and H2 are a result of the cross flow separating from the leeward side of the hull. There is a third vortex H3 that separates from the crease between the hull and the aft end of the deck casing.

The contour of axial vorticity in Figure 15 more clearly shows the arrangement of vortices on a lateral cross-section at midships ($x = 0$) for the $\beta = 10$ case. The same numbering is applied for the vortices behind the sail and sailplanes as for the zero incidence case, except with an additional identifier for port-side (P) or starboard side (S) as there is no-longer flow symmetry; 1P is the main sail-deck junction vortex that wraps around the port side of the sail, 4S is the primary sail tip vortex, and 13S and 13P are the tip vortices from the starboard and port sailplanes, respectively. The starboard leg of the primary sail-deck junction vortex (1S, not labelled) is difficult to identify because of the way it interacts with the hull separation vortex H2, which rotates in the opposite direction. The locations and magnitudes of peak axial vorticity for some of the vortex cores shown in Figure 15 are summarized in Table 9.

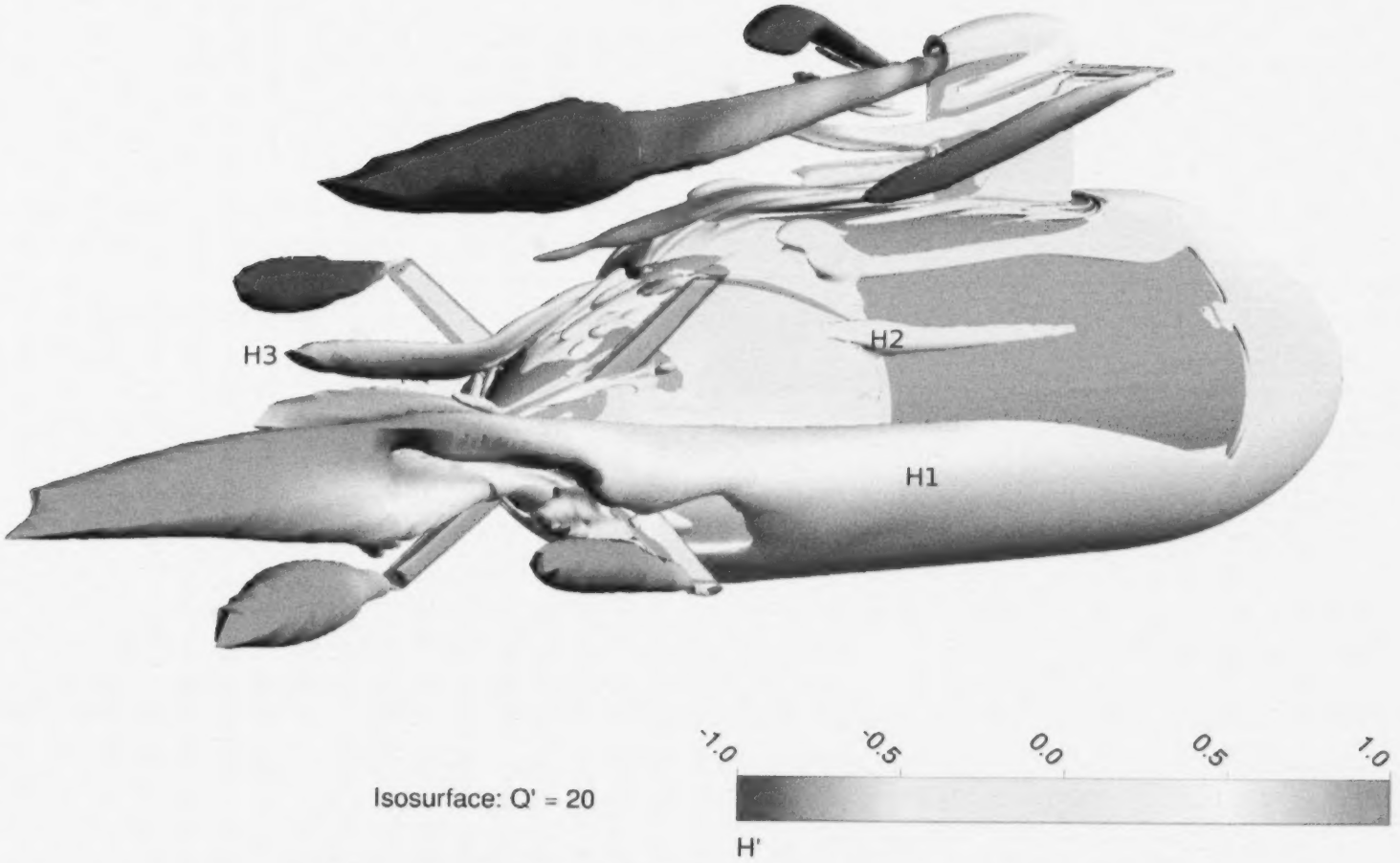

Figure 14: *Predicted vortex cores around the BB2 at* $\beta = 10°$.

Table 9: *Location and magnitude of maximum x-component of vorticity in the core of the vortices on the $x = 0$ plane, shown in Figure 15.*

Vortex #	y/L_{oa}	z/L_{oa}	$\omega_x L_{oa}/V_\infty$ Max
1P	0.00744	0.08898	84.71
4S	-0.01647	0.14237	328.22
13P	0.01953	0.15652	80.63
13S	-0.07201	0.12415	24.25

The accurate prediction of the separation lines and strengths of the hull vortices is important for predicting the hydrodynamic loads on the submarine [11]. An initial comparison between NATO AVT-301 participants' predictions showed a wide variation in the predicted vorticity magnitude in vortex cores as they progress downstream. As the next step going forward, a systematic verification study should be done to determine the mesh resolution required to obtain a mesh-converged converged solution. The results for different turbulence modelling approaches can then be compared.

In order to assess the current level of refinement through the primary sail tip vortex, a contour of the pressure coefficient, $c_p = P/(0.5\rho U^2)$, in the core region is overlaid with the mesh at two longitudinal positions in Figure 16. The radius of the vortex is taken to be the distance from the centre to the point of maximum circumferential velocity. Based on this definition, the $c_p = -0.4$ isoline for the midships cross-section in Figure 16 approximately defines the core of the vortex; this gives around 10 cells across the core. A study by Hally and Watt [13] found that approximately 10 cells across the core is adequate for propagating an idealized vortex with hexahedral cells aligned with the vortex axis. This indicates that the mesh refinement at midships is reasonable for capturing the sail tip vortex. However, additional cells may be need to achieve full mesh convergence because the cells are not perfectly aligned with the vortex due to the 10° drift angle. A follow on mesh refinement study should be done to assess this. At the propeller plane cross-section, the sail tip vortex passes through a block interface in the mesh where there is a significant increase in cell size. It is difficult to define the precise boundary of the vortex core but the large cells are on the order of 1/3 of the core diameter. This large cell size, combined with the large mesh expansion rate and misalignment between cells and the vortex axis should result in significant numerical diffusion. A similar assessment shows that the sailplane tip vortices are even less well resolved over the length of the submarine, with only around 2-3 cells across the core. These are areas of the mesh that should be improved/refined in the next stage of this project.

11.4 Surface pressure and shear stress

The predicted pressure and shear stress distributions on the BB2 are shown in Figures 17 and 18. An initial assessment of submissions from other participants indicates a good overall agreement in the pressure distribution but there are some difference in shear stress. In the

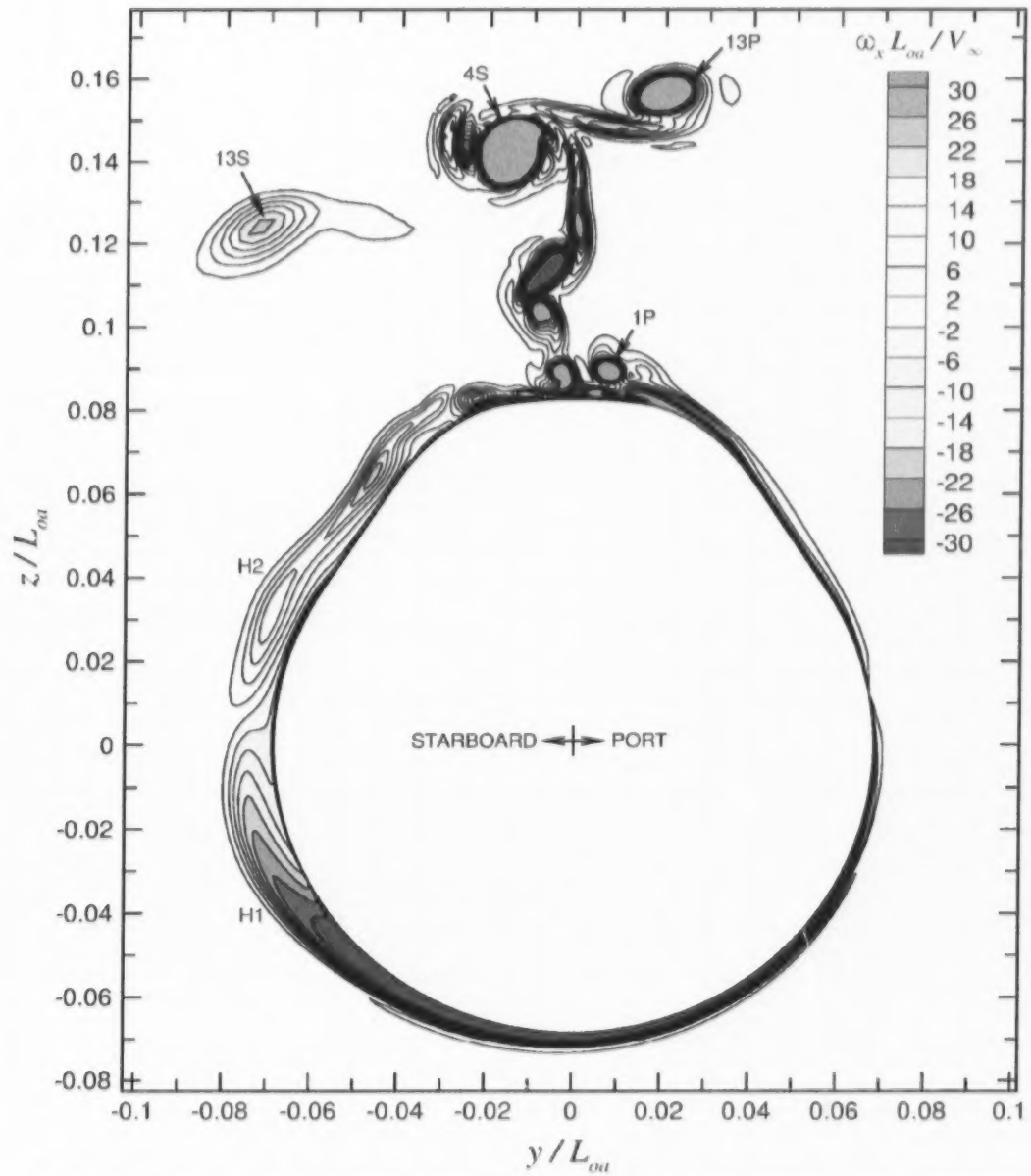

Figure 15: *Looking aft at vorticity contours on the $x = 0$ cross-sectional plane (located $0.060588 L_{oa}$ aft of sail trailing edge) for the $\beta = 10°$ case.*

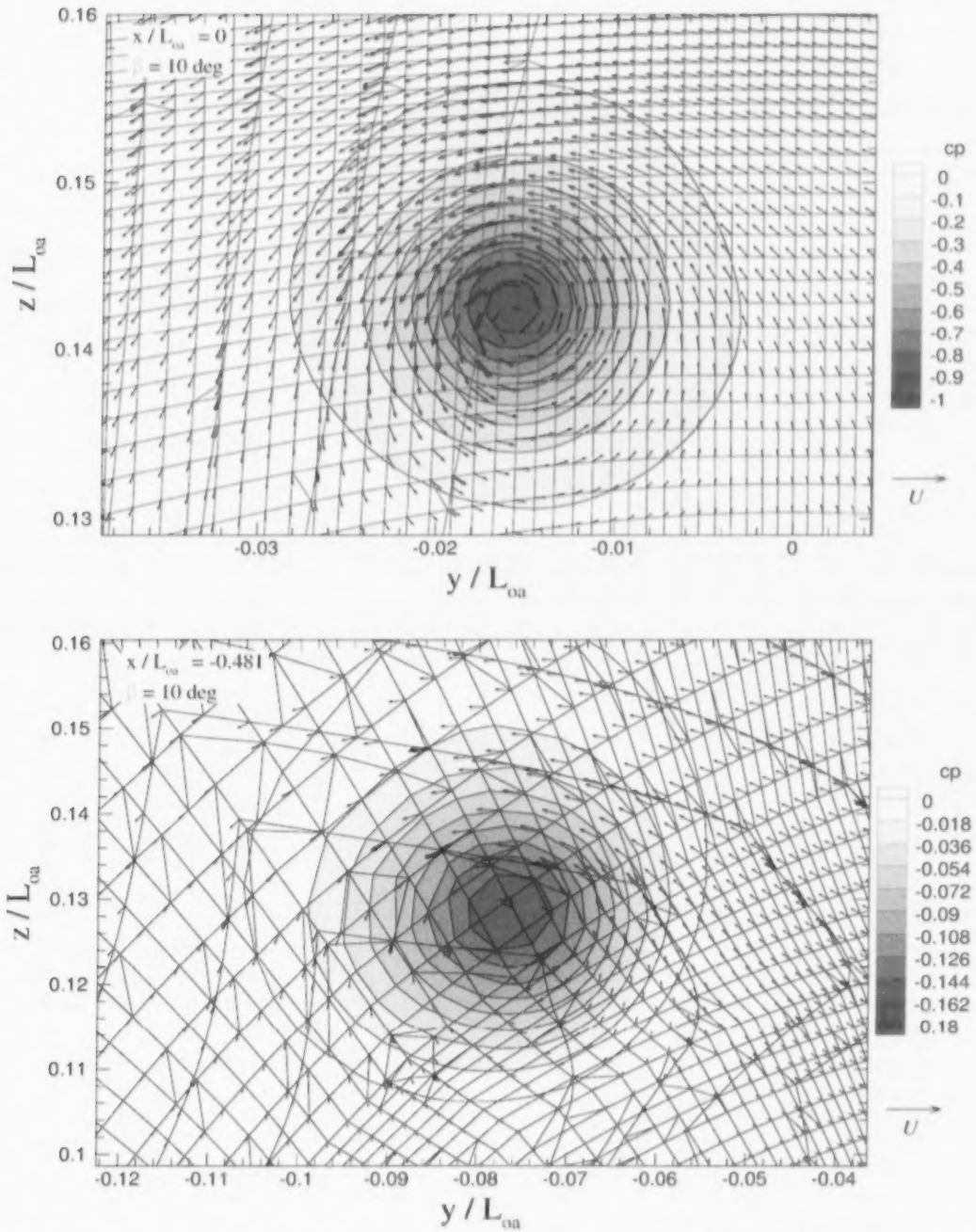

Figure 16: *Pressure through the primary sail tip vortex at midships ($x/L_{oa} = 0$) and the propeller plane ($x/L_{oa} = -0.481$), for the $\beta = 10°$ case.*

present DRDC calculations and some other submissions, the shear stress distribution has some high frequency noise that does not appear to be physical. The mesh should be verified to see if this is an issue with cells not conforming to the BB2 geometry or if there is an issue with the underlying CAD model. Also, the boundary layer is resolved well into the viscous sublayer in these calculations, with a computed average y^+ value of 0.0456, with a maximum value of 0.211 and standard deviation of 0.05. This allows the mesh to be used for a range of Reynolds numbers up to full-scale while still resolving the viscous boundary layer. However, the high cell aspect ratios at the BB2 surface make convergence more difficult and may be contributing to the noise in the shear stress prediction. Computations with a larger y^+ are planned for the next phase of this project.

11.5 Integrated Forces

The calculated hydrodynamic forces and moments are given in Tables 10 and 11. At zero incidence, the axial force is broken down into shear stress X'_s and pressure X'_p components. Due to the symmetry of the BB2 about the centre plane, the lateral force Y', yawing moment N', and rolling moment K' are all theoretically zero for zero flow incidence. The magnitude of all these normalized values were less than 1×10^{-9} at the end of the zero incidence RANS computation.

As expected, a large lateral force Y and large yawing moment N are predicted for the 10° drift case due to the crossflow drag on the hull and lift generated by the sail and tail planes. There is also a large rolling moment K because the centre of lift on the sail is above the hull axis. A significant out-of-plane force Z and pitching M are also predicted. As described by Watt et al. [14], these out-of-plane loads are due to the sail generating a flow circulation around the hull aft of the sail. This circulation interacts with the crossflow over the hull to generate a downward force over the aft end of the boat, which results in the nose-up pitching moment.

In the next phase of this project, a systematic grid refinement study will be conducted to determine the sensitivity of predicted hydrodynamics forces and moments on grid resolution.

Table 10: *Predicted BB2 hydrodynamic forces and moments for zero flow incidence, $Re_L = 9.57 \times 10^6$.*

X'_s	X'_p	X'	Z'	M'
-1.414×10^{-3}	-2.31×10^{-4}	-1.645×10^{-3}	-1.46×10^{-4}	-8.60×10^{-5}

Table 11: *Predicted BB2 hydrodynamic forces and moments for $\beta = 10°$, $Re_L = 9.57 \times 10^6$.*

X'	Y'	Z'	K'	M'	N'
-6.17×10^{-4}	-1.44×10^{-2}	-3.88×10^{-3}	4.68×10^{-4}	-6.39×10^{-4}	-3.32×10^{-3}

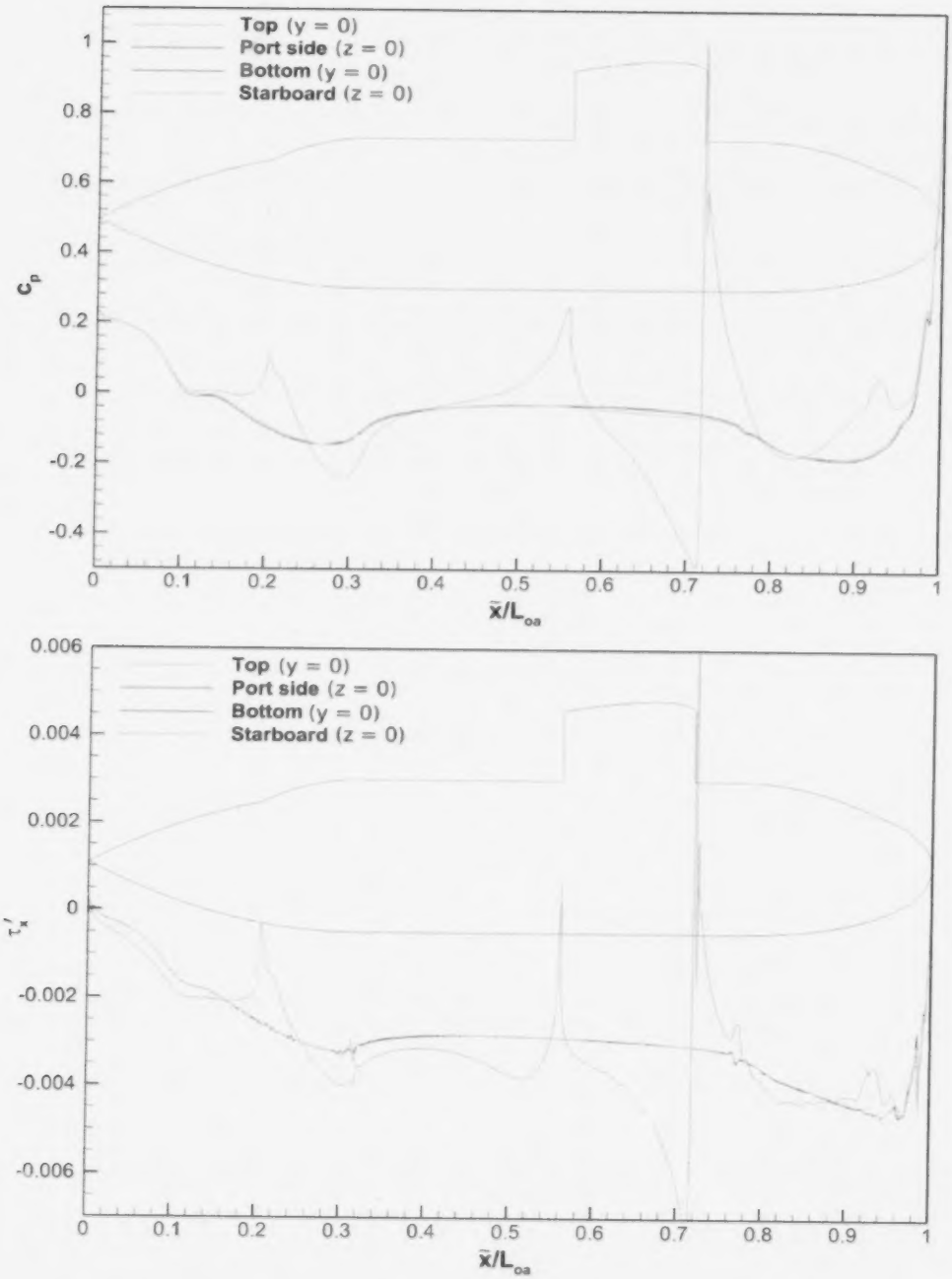

Figure 17: *Predicted pressure coefficient (top) and axial component of wall shear stress normalized by $0.5\rho U^2$ (bottom) along the BB2 for the zero incidence case.*

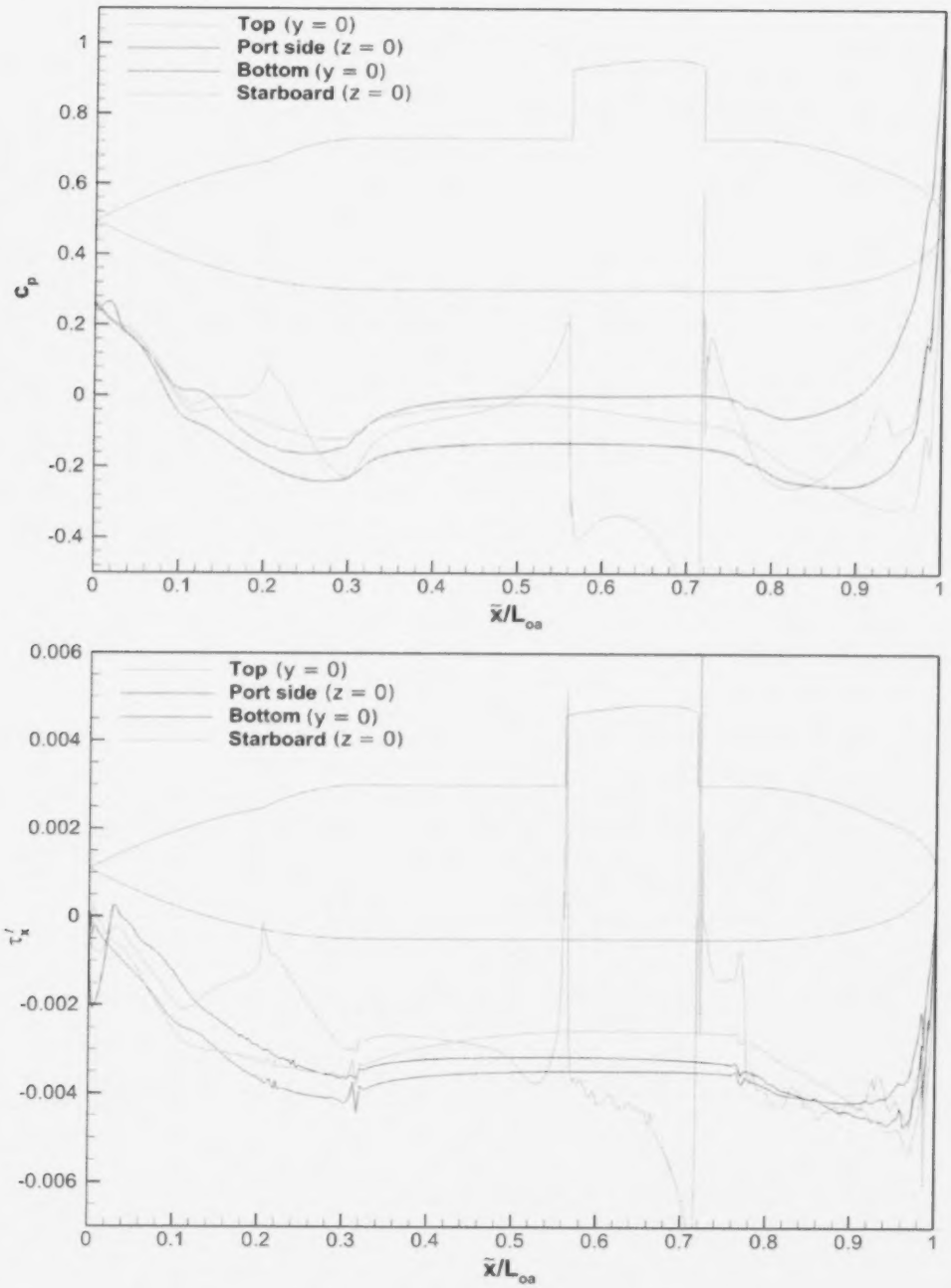

Figure 18: *Predicted pressure coefficient (top) and axial component of wall shear stress normalized by* $0.5\rho U^2$ *(bottom) along the BB2 for the* $\beta = 10°$ *case.*

12 Conclusions and future work

An initial 37 million cell structured mesh was created around the generic BB2 submarine model for the NATO AVT-301 collaborative project. Baseline RANS calculations were done on this mesh at zero incidence and 10° drift cases using the viscous flow solver ANSYS CFX with the Baseline Reynolds Stress turbulence model. Good iterative convergence could be obtained by alternating between large and small timestep sizes. A focus of the initial predictions was on resolving the sail horseshoe junction vortex. More work is needed to achieve adequate mesh resolution in this and other regions of the flow. The present calculations have identified the approximate size and location of vortices to guide subsequent mesh improvements. A strategy should be developed to refine regions with large gradients in flow variables, such as vortex cores, without incurring excessive computational cost. Some participants have found automatic mesh refinement methods to be very efficient; this should be investigated by DRDC. A systematic grid refinement study should also be done to assess numerical discretization errors.

Experience from phase zero will then be used to perform simulations at experimental conditions for wind tunnel experiments recently conducted by Australia. A comparison with different turbulence modelling approaches, such as a hybrid RANS large eddy simulations should also be considered in the future. Simulations of rotational submarine motion matching conditions for rotating arm experiments conducted by QinetiQ are also planned following the steady translation study.

References

[1] Overpelt, B., Nienhuis, B., and Anderson, B. (October, 2015), Free running manoeuvring model tests on a modern generic SSK class submarine (BB2), In *Pacific International Maritime Conference, Sydney, Australia.*

[2] Toxopeus, S. and Kerkvliet, M. (2017), NATO AVT-301 Collaborative Exercise: Part 1: Initial predictions for BB2.

[3] Joubert, P. N. (2006), Some aspects of submarine design - part 2. Shape of a submarine 2026, (Technical Report DSTO-TR-1622) Defence Science and Technology Organisation, Fishermans Bend, Victoria, Australia.

[4] Baker, C. R. (2006), A strategic meshing approach to modeling hydrodynamic flow around streamlined axisymmetric shapes, Masters thesis, Dept. of Mechanical Engineering, Univ. of New Brunswick.

[5] Hally, D. (2009), RANS calculations of the evolution of vortices on unstructured grids, (DRDC Atlantic TM 2009-052) Defence R&D Canada.

[6] ANSYS, Inc. (2016), ANSYS CFX-Solver Theory Guide, (Technical Report) SAS IP, Inc.

[7] Hutchinson, B., Galpin, P., and Raithby, G. (1988), Application of additive correction multi-grid to the coupled fluid flow equations, *Numer Heat Transfer*, 13(2), 133–147.

[8] Raw, M. J. (1994), A coupled algebraic multi-grid method for the 3D Navier-Stokes equations, In *Proceedings of the tenth GAMM-seminar. Notes on numerical fluid mechanics.*, Keil, Germany.

[9] Hutchinson, B. R. and Raithby, G. D. (1986), A multi-grid method based on the additive correction strategy, *Numerical Heat Transfer*, 9, 511–537.

[10] Raw, M. J. (1996), Robustness of coupled algebraic multi-grid for the Navier-Stokes equation., In *34th Aerospace and sciences meeting & exhibit*, Number AIAA 96-0297, Reno, NV.

[11] Jeans, T. L., Watt, G. D., Gerber, A. G., Holloway, A. G. L., and Baker, C. R. (2009), High-Resolution Reynolds-Averaged Navier-Stokes flow predictions over axisymmetric bodies with tapered tails, *AIAA Journal*, 47, 19–32.

[12] Toxopeus, S., Kuin, R., Kerkvliet, M., Hoeijmakers, H., and Nienhuis, B. (2014), Improvement of resistance and wake field of an underwater vehicle by optimising the fin-body junction flow with CFD, In *ASME 2014 33rd International Conference on Ocean, Offshore and Arctic Engineering*, Number OMAE2014-23784, San Francisco, CA.

[13] Hally, D. and Watt, G. D. (2002), RANS calculations of the evolution of vortices, (DRDC Atlantic TR 2001-216) Defence R&D Canada.

[14] Watt, G. D., Gerber, A. G., and Holloway, A. G. L. (2007), Submarine Hydrodynamics Studies Using Computational Fluid Dynamics, In *Proceedings of the eight Canadian Marine Hydrodynamics and Structures Conference*, St. John's, NL, Canada.

Annex A ANSYS CFX solver settings for the 10 degrees drift angle case

The following are the solver settings used for the ANSYS CFX simulation of the BB2 submarine model at a drift angle of 10 degrees, in CFX Command Language (CCL) format.

```
LIBRARY:
  CEL:
    EXPRESSIONS:
      Alpha = 0.0 [deg]
      Beta = 10 [deg]
      Lsub = 3.826 [m]
      NormForce = 0.5*Rho*Uinf^2*Lsub^2
      NormMom = 0.5*Rho*Uinf^2*Lsub^3
      Rho = 1000 [kg m^-3]
      Uin = -Uinf*cos(Beta)*cos(Alpha)
      Uinf = 3.0 [m s^-1]
      Vin = -Uinf*sin(Beta)
      Visc = 0.0012 [kg m^-1 s^-1]
      Win = Uinf*sin(Alpha)
      bf = step(aitern - 100.5) + (aitern-1)*0.01 * step(100.5 - aitern)
      dt = dtlg - (dtlg - dtsm)* (step(aitern-(ilg1)) * step((ilg1+ism) - \
        aitern) + step(aitern-(ilg1+ism+ilg)) * \
        step((ilg1+ilg+ism*2)-aitern) + step(aitern-(ilg1+ism*2+ilg*2)) * \
        step((ilg1+ilg*2+ism*3)-aitern) + step(aitern-(ilg1+ism*3+ilg*3)) * \
        step((ilg1+ilg*3+ism*4) - aitern) + step(aitern-(ilg1+ism*4+ilg*4)) \
        * step((ilg1+ilg*4+ism*5) - aitern) + \
        step(aitern-(ilg1+ism*5+ilg*5)) * step((ilg1+ilg*5+ism*6) - aitern) \
        + step(aitern-(ilg1+ism*6+ilg*6)) * step((ilg1+ilg*6+ism*7) - \
        aitern) + step(aitern-(ilg1+ism*7+ilg*7)) * step((ilg1+ilg*7+ism*8) \
        - aitern) + step(aitern-(ilg1+ism*8+ilg*8)) * \
        step((ilg1+ilg*8+ism*9) - aitern) + step(aitern-(ilg1+ism*9+ilg*9)) \
        * step((ilg1+ilg*9+ism*10) - aitern) + \
        step(aitern-(ilg1+ism*10+ilg*10)))
      ilg1 = 500
      ism = 300
      ilg = 15
      Nlrg = 50
      Nsm = 5000
      dtlg = Lsub/(Uinf*Nlrg)
      dtsm = Lsub/(Uinf*Nsm)
    END
  END
  MATERIAL: Fluid1
    Material Group = User
    Option = Pure Substance
    Thermodynamic State = Liquid
    PROPERTIES:
      Option = General Material
      EQUATION OF STATE:
        Density = Rho
        Molar Mass = 1.0 [kg kmol^-1]
        Option = Value
      END
      DYNAMIC VISCOSITY:
        Dynamic Viscosity = Visc
        Option = Value
      END
```

```
    END
  END
END
FLOW: Flow Analysis 1
  SOLUTION UNITS:
    Angle Units = [rad]
    Length Units = [m]
    Mass Units = [kg]
    Solid Angle Units = [sr]
    Temperature Units = [K]
    Time Units = [s]
  END
  ANALYSIS TYPE:
    Option = Steady State
    EXTERNAL SOLVER COUPLING:
      Option = None
    END
  END
  DOMAIN: FluidDomain
    Coord Frame = Coord 0
    Domain Type = Fluid
    Location = Assembly,Assembly 2
    BOUNDARY: Bottom
      Boundary Type = OPENING
      Location = Bottom,Bottom 2
      BOUNDARY CONDITIONS:
        FLOW REGIME:
          Option = Subsonic
        END
        MASS AND MOMENTUM:
          Option = Entrainment
          Relative Pressure = 0.0 [Pa]
        END
        TURBULENCE:
          Option = Zero Gradient
        END
      END
    END
    BOUNDARY: Inlet
      Boundary Type = INLET
      Location = In,In 2
      BOUNDARY CONDITIONS:
        FLOW REGIME:
          Option = Subsonic
        END
        MASS AND MOMENTUM:
          Option = Cartesian Velocity Components
          U = Uin
          V = Vin
          W = Win
        END
        TURBULENCE:
          Option = Low Intensity and Eddy Viscosity Ratio
        END
      END
    END
    BOUNDARY: Negy
      Boundary Type = OUTLET
      Location = Starboard
      BOUNDARY CONDITIONS:
        FLOW REGIME:
          Option = Subsonic
```

```
    END
    MASS AND MOMENTUM:
      Option = Average Static Pressure
      Pressure Profile Blend = 0.05
      Relative Pressure = 0 [Pa]
    END
    PRESSURE AVERAGING:
      Option = Average Over Whole Outlet
    END
  END
END
BOUNDARY: Outlet
  Boundary Type = OUTLET
  Location = Out,Out 2
  BOUNDARY CONDITIONS:
    FLOW REGIME:
      Option = Subsonic
    END
    MASS AND MOMENTUM:
      Option = Average Static Pressure
      Pressure Profile Blend = 0.05
      Relative Pressure = 0 [Pa]
    END
    PRESSURE AVERAGING:
      Option = Average Over Whole Outlet
    END
  END
END
BOUNDARY: Plusy
  Boundary Type = INLET
  Location = Starboard 2
  BOUNDARY CONDITIONS:
    FLOW REGIME:
      Option = Subsonic
    END
    MASS AND MOMENTUM:
      Option = Cartesian Velocity Components
      U = Uin
      V = Vin
      W = Win
    END
    TURBULENCE:
      Option = Low Intensity and Eddy Viscosity Ratio
    END
  END
END
BOUNDARY: Submarine
  Boundary Type = WALL
  Location = Hull,Sail,Sailplane,TailLS,TailUS,Hull 2,Sail 2,Sailplane \
    2,TailLS 2,TailUS 2
  BOUNDARY CONDITIONS:
    MASS AND MOMENTUM:
      Option = No Slip Wall
    END
    WALL ROUGHNESS:
      Option = Smooth Wall
    END
  END
END
BOUNDARY: Top
  Boundary Type = OPENING
  Location = Top,Top 2
```

```
    BOUNDARY CONDITIONS:
      FLOW REGIME:
        Option = Subsonic
      END
      MASS AND MOMENTUM:
        Option = Entrainment
        Relative Pressure = 0 [Pa]
      END
      TURBULENCE:
        Option = Zero Gradient
      END
    END
  END
  DOMAIN MODELS:
    BUOYANCY MODEL:
      Option = Non Buoyant
    END
    DOMAIN MOTION:
      Option = Stationary
    END
    MESH DEFORMATION:
      Option = None
    END
    REFERENCE PRESSURE:
      Reference Pressure = 0 [atm]
    END
  END
  FLUID DEFINITION: Fluid 1
    Material = Fluid1
    Option = Material Library
    MORPHOLOGY:
      Option = Continuous Fluid
    END
  END
  FLUID MODELS:
    COMBUSTION MODEL:
      Option = None
    END
    HEAT TRANSFER MODEL:
      Option = None
    END
    THERMAL RADIATION MODEL:
      Option = None
    END
    TURBULENCE MODEL:
      Option = BSL Reynolds Stress
    END
    TURBULENT WALL FUNCTIONS:
      Option = Automatic
    END
  END
END
INITIALISATION:
  Option = Automatic
  INITIAL CONDITIONS:
    Velocity Type = Cartesian
    CARTESIAN VELOCITY COMPONENTS:
      Option = Automatic with Value
      U = Uin
      V = Vin
      W = Win
    END
```

```
    STATIC PRESSURE:
      Option = Automatic with Value
      Relative Pressure = 0 [Pa]
    END
    TURBULENCE INITIAL CONDITIONS:
      Option = Medium Intensity and Eddy Viscosity Ratio
    END
  END
END
OUTPUT CONTROL:
  BACKUP DATA RETENTION:
    Option = Delete Old Files
  END
  BACKUP RESULTS: Backup Results 1
    File Compression Level = Default
    Option = Standard
    Output Equation Residuals = All
    OUTPUT FREQUENCY:
      Iteration Interval = 200
      Option = Iteration Interval
    END
  END
  MONITOR OBJECTS:
    MONITOR BALANCES:
      Option = Full
    END
    MONITOR FORCES:
      Option = Full
    END
    MONITOR PARTICLES:
      Option = Full
    END
    MONITOR POINT: Khull
      Coord Frame = Coord 0
      Expression Value = torque_x()@REGION:Hull + torque_x()@REGION:Hull 2
      Option = Expression
    END
    MONITOR POINT: Ksail
      Coord Frame = Coord 0
      Expression Value = torque_x()@REGION:Sail + torque_x()@REGION:Sail 2
      Option = Expression
    END
    MONITOR POINT: KspP
      Coord Frame = Coord 0
      Expression Value = torque_x@REGION:Sailplane 2
      Option = Expression
    END
    MONITOR POINT: KspS
      Coord Frame = Coord 0
      Expression Value = torque_x@REGION:Sailplane
      Option = Expression
    END
    MONITOR POINT: Ksub
      Coord Frame = Coord 0
      Expression Value = torque_x()@Submarine
      Option = Expression
    END
    MONITOR POINT: KsubNorm
      Coord Frame = Coord 0
      Expression Value = torque_x()@Submarine/NormMom
      Option = Expression
    END
```

```
MONITOR POINT: Ktail
  Coord Frame = Coord 0
  Expression Value = torque_x()@REGION:TailUS + \
    torque_x()@REGION:TailUS 2 + torque_x()@REGION:TailLS + \
    torque_x()@REGION:TailLS 2
  Option = Expression
END
MONITOR POINT: KtailLP
  Coord Frame = Coord 0
  Expression Value = torque_x()@REGION:TailLS 2
  Option = Expression
END
MONITOR POINT: KtailLS
  Coord Frame = Coord 0
  Expression Value = torque_x()@REGION:TailLS
  Option = Expression
END
MONITOR POINT: KtailUP
  Coord Frame = Coord 0
  Expression Value = torque_x()@REGION:TailUS 2
  Option = Expression
END
MONITOR POINT: KtailUS
  Coord Frame = Coord 0
  Expression Value = torque_x()@REGION:TailUS
  Option = Expression
END
MONITOR POINT: Mhull
  Coord Frame = Coord 0
  Expression Value = torque_y()@REGION:Hull + torque_y()@REGION:Hull 2
  Option = Expression
END
MONITOR POINT: Msail
  Coord Frame = Coord 0
  Expression Value = torque_y()@REGION:Sail + torque_y()@REGION:Sail 2
  Option = Expression
END
MONITOR POINT: MspP
  Coord Frame = Coord 0
  Expression Value = torque_y@REGION:Sailplane 2
  Option = Expression
END
MONITOR POINT: MspS
  Coord Frame = Coord 0
  Expression Value = torque_y@REGION:Sailplane
  Option = Expression
END
MONITOR POINT: Msub
  Coord Frame = Coord 0
  Expression Value = torque_y()@Submarine
  Option = Expression
END
MONITOR POINT: MsubNorm
  Coord Frame = Coord 0
  Expression Value = torque_y()@Submarine/NormMom
  Option = Expression
END
MONITOR POINT: Mtail
  Coord Frame = Coord 0
  Expression Value = torque_y()@REGION:TailUS + \
    torque_y()@REGION:TailUS 2 + torque_y()@REGION:TailLS + \
    torque_y()@REGION:TailLS 2
```

```
  Option = Expression
END
MONITOR POINT: MtailLP
  Coord Frame = Coord 0
  Expression Value = torque_y()@REGION:TailLS 2
  Option = Expression
END
MONITOR POINT: MtailLS
  Coord Frame = Coord 0
  Expression Value = torque_y()@REGION:TailLS
  Option = Expression
END
MONITOR POINT: MtailUP
  Coord Frame = Coord 0
  Expression Value = torque_y()@REGION:TailUS 2
  Option = Expression
END
MONITOR POINT: MtailUS
  Coord Frame = Coord 0
  Expression Value = torque_y()@REGION:TailUS
  Option = Expression
END
MONITOR POINT: Nhull
  Coord Frame = Coord 0
  Expression Value = torque_z()@REGION:Hull + torque_z()@REGION:Hull 2
  Option = Expression
END
MONITOR POINT: Nsail
  Coord Frame = Coord 0
  Expression Value = torque_z()@REGION:Sail + torque_z()@REGION:Sail 2
  Option = Expression
END
MONITOR POINT: NspP
  Coord Frame = Coord 0
  Expression Value = torque_z@REGION:Sailplane 2
  Option = Expression
END
MONITOR POINT: NspS
  Coord Frame = Coord 0
  Expression Value = torque_z@REGION:Sailplane
  Option = Expression
END
MONITOR POINT: Nsub
  Coord Frame = Coord 0
  Expression Value = torque_z()@Submarine
  Option = Expression
END
MONITOR POINT: NsubNorm
  Coord Frame = Coord 0
  Expression Value = torque_z()@Submarine/NormMom
  Option = Expression
END
MONITOR POINT: Ntail
  Coord Frame = Coord 0
  Expression Value = torque_z()@REGION:TailUS + \
    torque_z()@REGION:TailUS 2 + torque_z()@REGION:TailLS + \
    torque_z()@REGION:TailLS 2
  Option = Expression
END
MONITOR POINT: NtailLP
  Coord Frame = Coord 0
  Expression Value = torque_z()@REGION:TailLS 2
```

```
  Option = Expression
END
MONITOR POINT: NtailLS
  Coord Frame = Coord 0
  Expression Value = torque_z()@REGION:TailLS
  Option = Expression
END
MONITOR POINT: NtailUP
  Coord Frame = Coord 0
  Expression Value = torque_z()@REGION:TailUS 2
  Option = Expression
END
MONITOR POINT: NtailUS
  Coord Frame = Coord 0
  Expression Value = torque_z()@REGION:TailUS
  Option = Expression
END
MONITOR POINT: Xhull
  Coord Frame = Coord 0
  Expression Value = force_x()@REGION:Hull + force_x()@REGION:Hull 2
  Option = Expression
END
MONITOR POINT: Xsail
  Coord Frame = Coord 0
  Expression Value = force_x()@REGION:Sail + force_x()@REGION:Sail 2
  Option = Expression
END
MONITOR POINT: XspP
  Coord Frame = Coord 0
  Expression Value = force_x@REGION:Sailplane 2
  Option = Expression
END
MONITOR POINT: XspS
  Coord Frame = Coord 0
  Expression Value = force_x@REGION:Sailplane
  Option = Expression
END
MONITOR POINT: Xsub
  Coord Frame = Coord 0
  Expression Value = force_x()@Submarine
  Option = Expression
END
MONITOR POINT: XsubNorm
  Coord Frame = Coord 0
  Expression Value = force_x()@Submarine/NormForce
  Option = Expression
END
MONITOR POINT: Xtail
  Coord Frame = Coord 0
  Expression Value = force_x()@REGION:TailUS + force_x()@REGION:TailUS \
    2 + force_x()@REGION:TailLS + force_x()@REGION:TailLS 2
  Option = Expression
END
MONITOR POINT: XtailLP
  Coord Frame = Coord 0
  Expression Value = force_x()@REGION:TailLS 2
  Option = Expression
END
MONITOR POINT: XtailLS
  Coord Frame = Coord 0
  Expression Value = force_x()@REGION:TailLS
  Option = Expression
```

```
 END
 MONITOR POINT: XtailUP
   Coord Frame = Coord 0
   Expression Value = force_x()@REGION:TailUS 2
   Option = Expression
 END
 MONITOR POINT: XtailUS
   Coord Frame = Coord 0
   Expression Value = force_x()@REGION:TailUS
   Option = Expression
 END
 MONITOR POINT: XvsubNorm
   Coord Frame = Coord 0
   Expression Value = areaInt(Wall Shear X )@Submarine/NormForce
   Option = Expression
 END
 MONITOR POINT: Yhull
   Coord Frame = Coord 0
   Expression Value = force_y()@REGION:Hull + force_y()@REGION:Hull 2
   Option = Expression
 END
 MONITOR POINT: Ysail
   Coord Frame = Coord 0
   Expression Value = force_y()@REGION:Sail + force_y()@REGION:Sail 2
   Option = Expression
 END
 MONITOR POINT: YspP
   Coord Frame = Coord 0
   Expression Value = force_y@REGION:Sailplane 2
   Option = Expression
 END
 MONITOR POINT: YspS
   Coord Frame = Coord 0
   Expression Value = force_y@REGION:Sailplane
   Option = Expression
 END
 MONITOR POINT: Ysub
   Coord Frame = Coord 0
   Expression Value = force_y()@Submarine
   Option = Expression
 END
 MONITOR POINT: YsubNorm
   Coord Frame = Coord 0
   Expression Value = force_y()@Submarine/NormForce
   Option = Expression
 END
 MONITOR POINT: Ytail
   Coord Frame = Coord 0
   Expression Value = force_y()@REGION:TailUS + force_y()@REGION:TailUS \
     2 + force_y()@REGION:TailLS + force_y()@REGION:TailLS 2
   Option = Expression
 END
 MONITOR POINT: YtailLP
   Coord Frame = Coord 0
   Expression Value = force_y()@REGION:TailLS 2
   Option = Expression
 END
 MONITOR POINT: YtailLS
   Coord Frame = Coord 0
   Expression Value = force_y()@REGION:TailLS
   Option = Expression
 END
```

```
MONITOR POINT: YtailUP
  Coord Frame = Coord 0
  Expression Value = force_y()@REGION:TailUS 2
  Option = Expression
END
MONITOR POINT: YtailUS
  Coord Frame = Coord 0
  Expression Value = force_y()@REGION:TailUS
  Option = Expression
END
MONITOR POINT: Zhull
  Coord Frame = Coord 0
  Expression Value = force_z()@REGION:Hull + force_z()@REGION:Hull 2
  Option = Expression
END
MONITOR POINT: Zsail
  Coord Frame = Coord 0
  Expression Value = force_z()@REGION:Sail + force_z()@REGION:Sail 2
  Option = Expression
END
MONITOR POINT: ZspP
  Coord Frame = Coord 0
  Expression Value = force_z@REGION:Sailplane 2
  Option = Expression
END
MONITOR POINT: ZspS
  Coord Frame = Coord 0
  Expression Value = force_z@REGION:Sailplane
  Option = Expression
END
MONITOR POINT: Zsub
  Coord Frame = Coord 0
  Expression Value = force_z()@Submarine
  Option = Expression
END
MONITOR POINT: ZsubNorm
  Coord Frame = Coord 0
  Expression Value = force_z()@Submarine/NormForce
  Option = Expression
END
MONITOR POINT: Ztail
  Coord Frame = Coord 0
  Expression Value = force_z()@REGION:TailUS + force_z()@REGION:TailUS \
    2 + force_z()@REGION:TailLS + force_z()@REGION:TailLS 2
  Option = Expression
END
MONITOR POINT: ZtailLP
  Coord Frame = Coord 0
  Expression Value = force_z()@REGION:TailLS 2
  Option = Expression
END
MONITOR POINT: ZtailLS
  Coord Frame = Coord 0
  Expression Value = force_z()@REGION:TailLS
  Option = Expression
END
MONITOR POINT: ZtailUP
  Coord Frame = Coord 0
  Expression Value = force_z()@REGION:TailUS 2
  Option = Expression
END
MONITOR POINT: ZtailUS
```

```
        Coord Frame = Coord 0
        Expression Value = force_z()@REGION:TailUS
        Option = Expression
      END
      MONITOR POINT: ZvsubNorm
        Coord Frame = Coord 0
        Expression Value = areaInt(Wall Shear Z )@Submarine/NormForce
        Option = Expression
      END
      MONITOR RESIDUALS:
        Option = Full
      END
      MONITOR TOTALS:
        Option = Full
      END
    END
    RESULTS:
      File Compression Level = Default
      Option = Standard
      Output Equation Residuals = All
    END
  END
  SOLVER CONTROL:
    Turbulence Numerics = First Order
    ADVECTION SCHEME:
      Blend Factor = 1.0
      Option = Specified Blend Factor
      Gradient Relaxation = 0.1
    END
    CONVERGENCE CONTROL:
      Maximum Number of Iterations = 2000
      Minimum Number of Iterations = 10
      Physical Timescale = dt
      Timescale Control = Physical Timescale
    END
    CONVERGENCE CRITERIA:
      Residual Target = 1e-06
      Residual Type = MAX
    END
    DYNAMIC MODEL CONTROL:
      Global Dynamic Model Control = On
    END
    INTERPOLATION SCHEME:
      Pressure Interpolation Type = Trilinear
    END
  END
  EXPERT PARAMETERS:
    max solver its fluids = 60
    mg solver option = 5
    relax mass = 0.4
    solver relaxation fluids = 0.95
  END
END
COMMAND FILE:
  Results Version = 17.1
  Version = 17.1
END
```

Annex B ANSYS CFX solver settings for the zero incidence case

The zero incidence cases used the same solver settings as listed in Annex A, except for the following differences:

```
LIBRARY:
  CEL:
    EXPRESSIONS:
      Beta = 0 [deg]
      ilg1 = 200
    END
  END
END
FLOW: Flow Analysis 1
  BOUNDARY: Negy
    Boundary Type = OPENING
    Location = Starboard
    BOUNDARY CONDITIONS:
      FLOW REGIME:
        Option = Subsonic
      END
      MASS AND MOMENTUM:
        Option = Entrainment
        Relative Pressure = 0 [Pa]
      END
      TURBULENCE:
        Option = Zero Gradient
      END
    END
  END
  BOUNDARY: Plusy
    Boundary Type = OPENING
    Location = Starboard 2
    BOUNDARY CONDITIONS:
      FLOW REGIME:
        Option = Subsonic
      END
      MASS AND MOMENTUM:
        Option = Entrainment
        Relative Pressure = 0 [Pa]
      END
      TURBULENCE:
        Option = Zero Gradient
      END
    END
  END
END
SOLVER CONTROL:
  ADVECTION SCHEME:
    Gradient Relaxation = 0.01
  END
END
```

DOCUMENT CONTROL DATA

*Security markings for the title, authors, abstract and keywords must be entered when the document is sensitive

1. ORIGINATOR (Name and address of the organization preparing the document. A DRDC Centre sponsoring a contractor's report, or a tasking agency, is entered in Section 8.)

DRDC – Atlantic Research Centre
PO Box 1012, Dartmouth NS B2Y 3Z7, Canada

2a. SECURITY MARKING (Overall security marking of the document, including supplemental markings if applicable.)

CAN UNCLASSIFIED

2b. CONTROLLED GOODS

NON-CONTROLLED GOODS
DMC A

3. TITLE (The document title and sub-title as indicated on the title page.)

Baseline predictions of BB2 submarine hydrodynamics for the NATO AVT-301 collaborative exercise

4. AUTHORS (Last name, followed by initials – ranks, titles, etc. not to be used. Use semi-colon as delimiter)

Bettle, M. C.

5. DATE OF PUBLICATION (Month and year of publication of document.)	6a. NO. OF PAGES (Total pages, including Annexes, excluding DCD, covering and verso pages.)	6b. NO. OF REFS (Total cited in document.)
March 2018	42	14

7. DOCUMENT CATEGORY (e.g., Scientific Report, Contract Report, Scientific Letter)

Scientific Report

8. SPONSORING CENTRE (The name and address of the department project or laboratory sponsoring the research and development.)

DRDC – Atlantic Research Centre
PO Box 1012, Dartmouth NS B2Y 3Z7, Canada

9a. PROJECT OR GRANT NO. (If appropriate, the applicable research and development project or grant number under which the document was written. Please specify whether project or grant.)	9b. CONTRACT NO. (If appropriate, the applicable contract number under which the document was written.)
01EB	

10a. DRDC DOCUMENT NUMBER	10b. OTHER DOCUMENT NO(s). (Any other numbers which may be assigned this document either by the originator or by the sponsor.)
DRDC-RDDC-2017-R200	

11a. FUTURE DISTRIBUTION WITHIN CANADA (Approval for further dissemination of the document. Security classification must also be considered.)

Public release

11b. FUTURE DISTRIBUTION OUTSIDE CANADA (Approval for further dissemination of the document. Security classification must also be considered.)

Public release

12. KEYWORDS, DESCRIPTORS or IDENTIFIERS (Use semi-colon as a delimiter.)

Reynolds averaged Navier-Stokes (RANS); submarine; BB2; computational fluid dynamics (CFD); simulation

13. ABSTRACT/RÉSUMÉ (When available in the document, the French version of the abstract must be included here.)

Initial predictions of the hydrodynamic loads and flow field for the generic BB2 submarine model were computed using the commercial viscous flow solver ANSYS CFX with the Baseline Reynolds stress turbulence model (BSL-RSM). A block structured mesh having 37×10^6 cells was created for this purpose. Calculations were performed at a Reynolds number of 9.57×10^6 for steady translation with zero flow incidence and at a drift angle of $10°$. A strategy of alternating between large and small timesteps was found to be useful for converging the fluid equations for the wide range in time and length scales of vortices in the flow. The primary flow features around the BB2, such as junction vortices and appendage tip vortices, have been identified to guide future mesh improvements.

Nous avons calculé les prévisions initiales des charges hydrodynamiques et du champ d'écoulement du modèle générique de sous-marin BB2 à l'aide du résolveur commercial d'écoulement visqueux ANSYS CFX et du modèle de référence de turbulence à contraintes de Reynolds (BSL-RSM). À cette fin, nous avons créé un maillage structuré multibloc de 37×10^6 cellules. Les calculs ont été effectués à un nombre de Reynolds de 9.57×10^6 selon une translation constante à débit nul et un angle de dérive de $10°$. La stratégie qui consistait à alterner entre des intervalles de temps courts et longs s'est révélée utile à la convergence des équations des fluides dans une large gamme d'échelles de durées et de longueurs des tourbillons dans l'écoulement. Nous avons déterminé les principales caractéristiques de l'écoulement autour du BB2, telles que les tourbillons aux jonctions et à l'extrémité des appendices, ce qui orientera les améliorations à apporter au maillage à venir.